Chapter 2
Review of Literature

2.1 History of Aerogel

In 1931, Steven Kistler has introduced aerogel for the first time. Silica gel was used as the precursor material of aerogel. Aerogel was developed by increasing the pressure and temperature of the jellies beyond its critical point to replace the liquid of jellies with gas. A series of aerogels (silica, stannic oxide and cellulose) have been synthesized by Steven Kistler since first development (Kistler, 1931; Zheng et al., 2020). Though it was made clear since then that aerogel apprise with new amenities, the development of aerogel was restricted due to complexity in the development process. After few decades, researchers again paid attention to aerogel due to evolution of sol-gel method in combination with supercritical extraction (SCE) technology. Aerogels have been developed approximately nine decades ago however, the use of aerogel based compounds have increased greatly only a few decades ago. As aerogel possess superior qualities, researcher showed their interest in the development process of aerogel (Nita et al., 2020). Poly vinyl alcohol (PVA), polysaccharides, proteins, seed mucilage, etc. based aerogel are quite common nowadays. Mainly, the trend is going towards bio-based aerogel as these are biodegradable, non-toxic and less hazardous.

2.2 Development of Aerogel

Fabrication of aerogel is a four stage procedure (**Fig. 2.1**) which includes first solution making stage, second hydrogel formation stage, third alcogel formation stage and finally fourth aerogel formation stage. This process is commonly used to fabricate both organic (polysaccharides, proteins etc.) and inorganic (silica, titanium dioxide etc.) aerogel. Firstly, a water based solution is prepared with the precursor material and then it is formed into a hydrogel using a cross-linking promoter compound. Then, the hydrogel is converted to alcogel by substituting the water present in hydrogel with alcohol (commonly ethanol). Eventually, alcohol is extracted from alcogel by drying (supercritical, vacuum, ambient pressure, etc.) and the aerogel is obtained (García-González et al., 2011). The drying process act as deciding factor whether the additional alcogel preparation is required or not. Freeze drying does not need to follow alcogel preparation step as it can make aerogel directly from hydrogel.

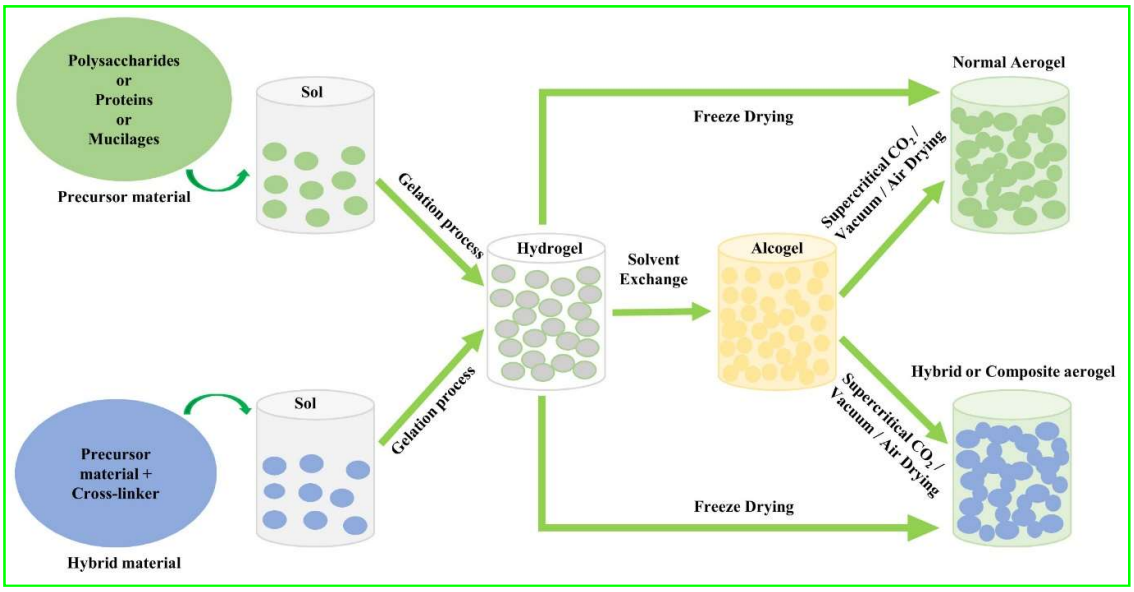

Fig. 2.1 Necessary steps involved in the development of aerogel

2.2.1 *Preparation of Gel*

An aqueous solution of precursor mterial or water swollen hydrogel (**Fig. 2.1**) is formed at the starting point. However, in some cases organic solvents (lyogels) are used to form aerogel (cellulose gel in NMMO (N-methylmorpholine-N-oxide) solvent). The degree of crosslinking between the polymer chains determines the 3D structure of the gel. To obtain high performance aerogel, proper selection of precursor material, functional group of precursor material, pH, and cross-linker content is important (Favaro et al., 2008). Depending upon the nature of cross-linking hydrogels are categorized as physical or chemical hydrogel. Weak forces due to ionic interactions, hydrogen bonding etc. forms a reversible crosslink between polymeric chains in physical hydrogel. In chemical hydrogels cross-linking promoters (sucrose, glutaric acid etc.) are used to stengthen the polymer chains by forming covalent bond (García-González et al., 2011). Upto a threshold value, the cross-linker content increases total pore volume and surface area of final aerogel. However, cross-linking with faster kinetics leads to form non-homogeneous gel structure (Alnaief et al., 2011). Therefore, choice and concentration of cross-linker is important which can alter the aerogel stability, homogeneity and open porosity.

2.2.2 *Solvent Exchange*

Solvent exchange is the next important stage of aerogel preperation in which hydrogel is converted into alcogel (**Fig. 2.1**). It has been done before supercritical drying of gel. Supercritical drying is performed using supercritical carbon dioxide ($SCCO_2$). The solvent exchange is performed due to lower affinity of water to $SCCO_2$. Most commonly, acetone or

alcohol is used as substitute of water due to their high solubility in CO_2 (Stievano & Elvassore, 2005). Solvent exchange is performed either by following a single step procedure or by following a multi step procedure. In single step procedure, gel is soaked directly in the target solvent and in multi step procedure, soaking is done by dipping the gel in water-to-target solvent mixture of different concentration (target solvents concentration is increased with time in a stepwise manner) (Robitzer et al., 2008). Moreover, solvent is selected upon fulfilling some required criterias like (i) gel structure must not be dissolved by it, (ii) completely soluble in it, and (iii) accepted for food and pharmaceutical application. However, shrinkage takes place in polysaccharide based aerogels in this step therefore, special attention must be required (García-González et al., 2011; Mehling et al., 2009).

2.2.3 *Drying of Gel*

Drying is the final and important stage (**Fig. 2.1**) of aerogel development as drying influences the structural network of solid, functional properties, mechanical and physical properties of the aerogel. Capillary pressure gradient (100-200 MPa, able to collapse the pores) inside the gel nanopores is created due to surface tension as a consequence of solvent removal (García-González et al., 2011). To preserve the connected structure from shrinkage, direct evaporation of liquid is avoided (Zheng et al., 2020). Therefore, proper selection of drying method is very important while fabricating aerogels as crack formation is unavoidable (Jin et al., 2004). Freeze drying and $SCCO_2$ drying is mostly used however, in some cases air drying method is also used (Nita et al., 2020).

2.2.3.1 *Freeze drying*

It is one of the widely adopted techniques of aerogel manufacturing. Generally, it is a two step procedure, the first step consists of pre-freezing (temperature ranges between -45 °C to -15 °C) of the wet gel material to get converted it into a solid state and the second step consists of sublimation which converts the liquid (present in solid state) in to gas under vacuum. The second step leads to the formtion of pores inside the aerogel matrix (Ni et al., 2016; Wang, Chen, et al., 2019). In pre-freezing stage, the volume increase due to ice crystal formation from the liquid leads to shrinkage and breakge in crust layers. Moreover, the growth rate of ice crystals are not same which results in non-homogeniety in pore structure of aerogel (Zheng et al., 2020). Nevertheless, solute molucules are pushed inside the ice crystal unavoidably during pre-freezing (Wang, Chen, et al., 2019). Freeze drying technique was used to produce soy protein-nanocellulose composite aerogel (frozen at -10 °C; (Arboleda et al., 2013)), alginate/pectin aerogel (frozen at -80 °C for 48 h, freeze dried at a condensor tempearture -58

°C under vaccum (< 5 Pa) for 48 h; (Chen & Zhang, 2019)), cellulose based aerogels from Arundo donax waste biomass (frozen at -80 °C; (Fontes-Candia et al., 2019)) etc. The whole process is energy intensive, expensive and time consuming (more than 10 h; (Zheng et al., 2020)). Agglomeration can takes place as a consequence of freeze drying (Abdul Khalil et al., 2020).

2.2.3.2 *Supercritical drying*

It is a widely accepted technique for drying of alcogel. Supercritical fluids are having pressure and temeperature beyond the critical range of those fluids. They exhibit properties of liquid (density, dissolving capacity etc.) as well as gas (diffusion coefficient is high, viscosity is less etc.). Without any gas-liquid interface and surface tension, solvent strength and density of supercritical fluids are adjustable (García-González et al., 2012). Among all supercritical fluids $SCCO_2$ is widely used due to its special characteristics like, low cost, easily available, non-toxic, chemically inert, mild operating conditions needed to reach critical point (temperature: 31.1 °C and pressure: 7.4 MPa), and non-combustible (Ubeyitogullari & Ciftci, 2017). Nevertheless, during drying it minimizes the interaction and conformation of molecular chains of the network (Garćia-González, Alnaief & Smirnova, 2011). In $SCCO_2$ drying primarily, the high dissolution of $SCCO_2$ in liquid gel solvent expanded the liquid and as a consequence of volume expansion of the liquid spillage takes place from the gel network. Then, over time CO_2 content is increased in pore gel liquid till CO_2 reaches to critical condition. Eventually, $SCCO_2$ substitute the liquid without any collapse in the gel network (due to absence of surface tension) and transitted into vapor state to form the required aerogel (Garćia-González, Alnaief & Smirnova, 2011). $SCCO_2$ drying (pressure 200 bar, temperature 45 and 35 °C respectively, drying time 5 h) technique was used to produce maize starch aerogel and calcium alginate aerogel (Franco et al., 2018), protein (whey protein isolate, egg white protein and sodium caseinate) based aerogel (temperature 45 °C, pressure 12 MPa, drying time 6 h; Kleemann et al., 2018; Selmer et al., 2019), pectin based nanocomposite aerogel (temperature 50-60 °C, pressure 11-13 MPa, drying time 5 h; Nešić et al., 2018), etc. However, this technique is expensive and complicated (Abdul Khalil et al., 2020).

2.2.3.3 *Air drying*

Air drying technique is also used in the drying of alcogel. The drying is performed at ambient temperature and pressure or in oven at constant temperature until it reaches to a constant weight (Ubeyitogullari, Brahma, Rose, & Ciftci, 2018). During air drying, direct evaporation of solvent takes place which leads to generate capilliary tension (100-200 MPa)

and when th solvent is emptied form gel network it contracts the pores due to recede of liquid-vapor meniscus formed inside the pores (Zheng et al., 2020). Air drying technique was used to produce nanoporous wheat starch aerogels (temperature 21 °C; Ubeyitogullari, Brahma, Rose, & Ciftci, 2018), carbon aerogels based on potato, maize and rice starches (temperature 50 °C, drying time 24 h; Bakierska et al., 2017) . It is an easy technique of drying however, it is very time consuming (more than 48 h) (Bakierska et al., 2017; De Souza et al., 2014).

2.2.3.4 *Microwave drying*

Microwave drying is another important drying technique which results aerogel with suitable porosity and high specific surface area (SSA). Aerogel developed using these technique exhibits comparable morphological structure with small interconnected pores (Zuo et al., 2015). Microwave imparts alternating electromagnetic field which causes rotation of liquid molecules and align their electric dipoles which promotes overall molecular vibration and thereby promotes their own heating. Therefore, high temperature heating cycle is also avoided. Microwave drying possesses some advantages like, smaller thermal gradients as it generates heat internally, fast and uniform heating, reduced drying time and energy consumption etc. (Durães et al., 2013). This drying technique (450 W -three cycles of two minutes each at an interval of two minutes) was used to produce aerogel like material from methyltrimethoxysilane (MTMS) precursor (Durães et al., 2013). Moreover, it's a very time saving and sustainable method as it is simple, rapid, energy efficient, environment friendly, etc.

2.3 Types of Aerogel

Traditionally, inorganic materials (silica, titanium, graphene etc.) are used to make aerogels and these aerogel are used for non-food applications (double-pane windows) due to their transperancy and thermal insulation capacity. Afterwards, organic materials (resorcinol formaldehyde polymers) also comes into picture due to their stiffness and strength (Mikkonen et al., 2013). Moreover, biopolymers (polysaccharides, starch, protein etc.) are used to develop aerogels for different food and non-food application. Biopolymer based aerogels have achieved a huge acceptance due to their biodegradibility, biocompatibility and food application. Nowadays, nanomaterials are incorporated within the solid materials to provide desired applications (nutritional, anti-microbial etc.). Therefore, based on the solid material characteristics aerogels (**Fig. 2.2**) are classified as inorganic and organic aerogels (Nita et al., 2020). However, based on the precursor materials food grade aerogels can be called as starch based aerogels, protein based aerogels, cellulose based aerogels etc (Selvasekaran and Chidambaram, 2021).

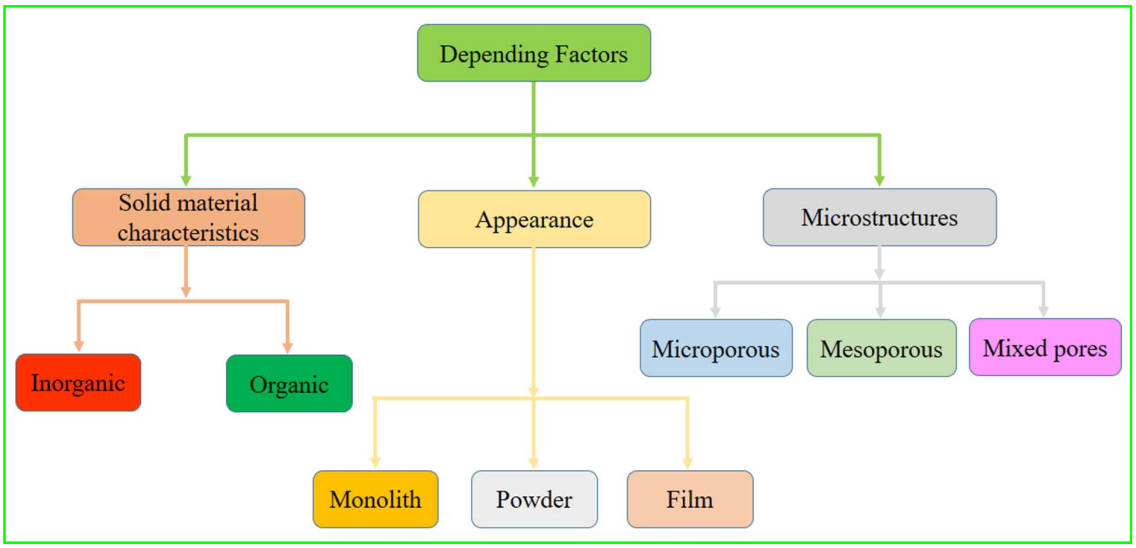

Fig. 2.2 Types of Aerogel

2.3.1 *Inorganic Aerogel*

Since, the ancient times inorganic aerogel have developed and used. Inorganic aerogel are those in which inorganic materials are used as the structural solid materials. These inorganic materials can be fluoride (AlF_3), silica (native and hybrid), oxides (SiO_2, TiO_2, SnO_2, Al_2O_3 etc.), chalcogens (CdS, ZnS, PbS etc.) and metals (Pt, Au, PtAg etc.) (Nita et al., 2020). Inorganic aerogels are used majorly in non-food areas (packaging, thermal insulation etc.). Nevertheless, under small stresses, inorganic aerogel subject to collapse as a consequence of lacking mechanical strength.

2.3.2 *Organic Aerogel*

To overcome the problem of fragility in inorganic aerogel, organic aerogel have developed. Organic aerogel are reported as stronger aerogel than the inorganic aerogel (Mavelil-sam et al., 2018). By definition, organic aerogel are those in which organic materials are used as the structural solid materials. Organic aergels can be of carbon based (cryogel) and polymer based (synthetic and biopolymer). Melamin, resorcin, PVA etc. are most commonly used synthetic polymers in aerogels. Polysaccharides, cellulose, starch, alginate, proteins etc. are majorly used biopolymers in organic aerogel (Nita et al., 2020). Among those biopolymer based aerogel have gained importance due to their biodegradibility, biocompatibility, non-hazardous and environment friendly nature.

Nevertheless, based on apperance and microstructures, aerogel can be classified as monolith, powder and film and microporous, mesoporous and mixed pores respectively (**Fig. 2.2**). Further biopolymer based aerogel were discussed in **section 2.5** in detail.

2.4 Properties of Aerogel

2.4.1 *Density and porosity*

Porosity can be calculated from aerogel density. Density and porosity of aerogels largely depends on the precursor material, aerogel making procedure and the cross-linking material used (Abdul Khalil et al., 2020). A drastic change in density and porosity takes place when aerogels are formed from hydrogels. This may be due to air substitution in the place of liquid (Zaman et al., 2020). Density is directly proportional to the initial concentration of the precursor material and inversly proportional to porosity (Zaman et al., 2020; Abdul Khalil et al., 2020). Density of aerogels are strongly influenced by concentration of precursor materials , the expansion of dispersion during gel formation and the volumetric shrinkage during solvent exchange and drying of alcogel (Lavoine and Bergström, 2017). The porosity of aerogels can be higher than 99 %. Maintaining a percolative network and cross-linking of polymer matrix leads to reduction in shrinkage. However, porosity and pore size is less in aerogels containing higher amount of fibre in the solid network. Moreover, forced drying leads to collapse in aerogel network. However, moist drying (20 °C and 50 % relative humidity), solvent exchange at low temperature (-20 ° C) followed by $SCCO_2$ drying, can prevent shrinkage and preserve the porous network (Lavoine and Bergström, 2017; Abdul Khalil et al., 2020).

2.4.2 *Specific surface area*

Specific surface area (SSA) is a critical parameter which represents the microstructural characteristics of aerogel (Zhu, 2019). In aerogels, a high SSA is always needed for their applications. To obtain high SSA in aerogels, pore closure must be avoided through exchanging water with tert-butanol (TBA) and good dispesibility of precursor materials should be maintained (Lavoine and Bergström, 2017; Abdul Khalil et al., 2020). Sehaqui, Zhou and Berglund (2011) reported high SSA (maximum 284 m^2/g) of aerogels after successful replacement of water with TBA. Moreover, Lavoine and Bergström (2017) suggested that nanomaterials (nano-cellulose) did not form dense bundles or aggregrate with the increasing concentration. Chen et al. (2014) reported largest SSA in the range of 500 to 600 m^2/g in nano-cellulose based aerogel developed through $SCCO_2$ drying). Large SSA with high porosity

contributes to high capacity of absorption and high loading capacity of bioactive components (Mi et al., 2018; Wan et al., 2019; de Oliveira et al., 2020).

2.4.3 *Morphology and pore size*

The method of preparation and the initial concentration of precursor material influences the pore size of aerogels. However, the morphology of aerogels are influenced by physical conditions, precursor material, method of preparation, cross-linking or additive materials and rate of cooling (Abdul Khalil et al., 2020). Moreover, porosity of aerogel also influences the morphology (de Oliveira et al., 2020). Pore size and morphology of aerogels have great impact on thermal and mechanical properties. Supercritical drying is commonly used to obtain small (<50 nm) and open pores in nanocellulose-based aerogels. However, ice templating provides nanocellulose-based aerogel with open pores having diameter ≥50 nm. Nevertheless, rapid cooling provides more organized and homogeneous structure with smaller pores (1-60 nm). As the concentration of precursor material is increased, pore size is decreased and more regular structure is found (Lavoine and Bergström, 2017; Abdul Khalil et al., 2020). Addition of cross-linking materials modifies the microstucture of aerogels and provide uniformity to the pore distribution of aerogels. Hence, provides stability to the aerogel by strengthening the hydrogel network (Abhari, Madadlou, and Dini, 2017; Zhu, 2019). Oliveira, Bruni, El Halal, et al. (2019) reported more organized aerogel structure and interconnected pores in rice cellulose nanocrystals based aerogel than oat cellulose nanocrystal based aerogel. The pore size and pore distribution is crucial parameters in food packaging as they regulates the quantity and mechanism of absorption of water since small pores possess lower water absorption ability (Oliveira, Bruni, El Halal, et al., 2019).

2.4.4 *Water absorption capacity*

To verify how aerogels acts as water absorber after 24 hours, water absorption capacity (WAC) is analyzed. Das et al. (2014) reported that when water firstly comes in contact with dry aerogels, water is readily absorbed by the polar molecules and the polymer structure is increased after hydration. After hydration water is exposed to hydrophobic molecules and interaction of water and hydrophobic groups takes place as a consequence of expnsion in structure and hydration. The interaction and covalent force maintains the structure and provide elasticity to the aerogel. Moreover, when water absorption and retention forces are balanced, the maximum water absorption will be achieved by the aerogel. Low density and high SSA of aerogel made them capable of exhibiting high absorption capacity (Mi et al., 2018). The porous structure of aerogel network and the characteristics of precursor materials influences the water

absorption capacity of aerogels. High value of water absorption capacity may be attributed to the hydrophilic nature of precursor materials. Moreover, cellulose/nanocellulose incorporated aerogels exhibited more open and porous (3D) structure with higher SSA which collectively enhances absorption capacity and loading capacity of bioactive compounds (de Oliveira et al., 2020). Moreover, Mikkonen et al. (2013) reported that high surface area and the presence of functional groups in polysaccharides based aerogel leads them easily available for interactions with the compunds (water, water vapor etc.) of surrounding environment. Water absorption through capillary force in polysaccharide based aerogel is reported by Mallepally et al. (2013). Oliveira, Bruni, El Halal, et al. (2019) reported water absorption capacity ranged from 264.2 to 402.8 % of cellulose nanocrystal based aerogels. It has also reported that the higher water absorption capacity of oat cellulose nanocrystals based aerogels is due to bigger pore size compare to other cellulose nanocrystals based aerogels. High water absorption capacity is desirable in food packaging applications (example: meat) as it reduces condensation of moisture and water activity which indirectly protect the food from microbial spoilage (de Oliveira, Bruni, El Halal, et al., 2019).

2.4.5 *Mechanical and thermal properties*

Mechanical properties of aerogel are closely related to the microstructure and morphology of the aerogel network (Zhu, 2019; Abdul Khalil et al., 2020). Moreover, mechanical properties are also influenced by the charateristics of the precursor material (Cheng et al., 2012; Mikkonen et al., 2013). Aerogel network containing larger size pores exhibit lower mechanical strength. However, densed network of precursor material inside the aerogels displays more organized and homogeneous structure which results in low porosity and high mechanical strength to withstand heavy load (Zheng et al., 2017; Zaman et al., 2020).Cellulose/nanocellulose based aerogels exhibit good mechanical properties in terms of compressive strength, flexibility, toughness, high modulus etc. (Zaman et al., 2020). Incorporation of nanomaterials (CNF:cellulose nano fibre) in polymer matrix increases the mechanical strength of aerogel due to increase in SSA of interaction within the polymer matrix (Abdul Khalil et al., 2020). Desirable mechanical strength in aerogel is required for food packaging application. Nowadays, biopolymer based aerogel (cellulose, polysaccharides etc.) are preferred due to their higher strength and biodigradibility (Ramesh et al., 2017; Abdul Khalil et al., 2020).

Thermal conductivity is the main component under thermal properties of aerogel. Thermal conductivity of an aerogel is contributed by: (i) conduction through the solid (λ_{solid}); (ii) conduction through the gas (λ_{gas}); (iii) convection within the cells; and (iv) radiation through

the cell walls and across the cell voids (λ_{rad}). However, convection through the gas is dominated by conduction through the gas hence, convection is neglected (Lavoine and Bergström, 2017). Generally, aerogel have low thermal conductivity which may be attributed to low density and greater mean free path length of air molecules than very small size pores (Koebel, Rigacci, and Achard, 2012; Zhu, 2019). Thermal conductivity is scaled by the density of the aerogel. As the density is decreased (37 to 17 mg/cm^3), thermal conductivity is also decreased (0.04 to 0.018 W/m-K). In composite materials, *kapitza* resistance (interfacial thermal resistance) plays an important role in reducing the thermal conductivity (Kobayashi et al., 2014; Lavoine and Bergström, 2017). Moreover, it increases with the increase in cell size and decreases with the increase in relative density. Nevertheless, with the increasing density thermal conductivity is also increased in aerogels having high SSA and small pore (≈ 30 nm) (Lavoine and Bergström, 2017). Basically, thermal conductivity is desired in food packaging application to safeguard the food from spoilage due to heating. Thermal stability is another aspect of thermal properties of aerogels. This concept is utilized in applications like microwavable food packaging. Nanofibrillated cellulose (NFC) aerogels can withstand upto 275 °C before starting degradation whereas, starch based aerogels starts to degrade at 280-330 °C. The more the open structure, the more the efficient heat penetration (Mikkonen et al., 2013; Zhu, 2019).

2.4.6 *Antioxidant properties*

Bioactive compounds having antioxidant potential is incorporated inside the aerogel matrix to provide antioxidant activity to the aerogel. Aerogels are used as carriers which largely excavate the solubility and bioavailability of those bioactive compounds. Impregnation process is being used to encapsulate those bioactive compounds. The size of bioactive compunds are reduced, while solubility is increased due to impregnation process (Zhu, 2019). Antioxidant activity analysis has carried out to obtain bioactivity of aerogels. However, it is noteworthy mentioning that antioxidant activity of a pure substance is greater than in bioactive aerogels. Moreover, the method of preparation has impact on antioxidant properties of bioactive aerogels. Physical crosslinking and freeze drying have negligible impact on antioxidant activity (de Oliveira et al., 2020). Nevertheless, precursor materials interaction with the encapsulated compounds influences the antioxidant activity. Hu et al. (2015) describes that the presence of nanocellulose as filler into the aerogel matrix made yerba-mate based extract (YMBE) less available for interaction with DPPH hence, a small decrease in antioxidant activity was observed. Gullón et al. (2018) reported that yerba-mate products consists of polysaccharides, proteins, vitamins, minerals, alkanoids, polyphenols, flavonoids etc. hence, they provide good

antioxidant activity against free radicals. Therefore, encapsulation of bioactive compound in precursor materials exhibit good potential for formulation of food preservatives and nutraceuticals (de Oliveira et al., 2020). The release kinetics of bioactive compounds is of great importance in food packaging application. Slow, gradual and easy release of materials are highly recommended in food presevation and active package (de Oliveira et al., 2020). The SSA is considered as a crucial factor which controls the dissolution rate and absorption of compounds. Aerogels having hydrophilic nature, rapidly release compounds (aerogels made with neat poly vinyl alcohol) (Dai et al., 2019). Moreover, precursor material (cellulose) can also influence the release rate due to their own characteristics (being an hydrophilic material exhibits contolled release due to presence of pyranose rings which possess hydrophobic character). Hence, selection of encapsulating material is very important as it regulates safe and adequate release of encapsulated material in food matrix (Bora et al., 2018; de Oliveira et al., 2020).

2.5 Bio-polymer based Aerogel

2.5.1 *Polysaccharide based aerogel*

Polysaccharides are the most abundant carbohydrates found in food. Polysaccharides are formed by binding the monosaccharide units with glycosidic linkages. Cellulose, hemicellulose, starch, chitosan, carrageenan, alginate, pectin etc. are some common form of polysaccharides. Now a days polysaccharides are used to make aerogels due to their quality traits (light weight, large SSA and very porous: porosity 90-99 %), ease of availability, bioactivity, non-toxicity, environment friendly nature (biocompatibility and biodegradibilty), and sustainability. Moreover, polysaccharides are acquianted for their capability to order or assemble themselves into certain forms or structures (Nita et al., 2020). Some of the polysaccharides precursor based aerogel (**Table 2.1**) are discussed below.

2.5.1.1 *Cellulose based aerogel*

Cellulose is one of the most common form of polysaccharide and it is one of the most abundant source of polysaccharides available. Cellulose can be derived from low cost biomass which made them economic source of precursor material of aerogel. Plants primary and secondary cell wall contains 9-25 % and 40-80 % cellulose. At the early stages, cellulose were used in silica-based aerogel. Now a days, cellulose as a renewable, biodegradable and biocompatible source, is used individually to prepare aerogel (**Table 2.1**) with large SSA and high porosity. Nanocellulose is referred as the nano-structured cellulose materials.

Furthermore, nanocelluloses are derived from cellulose by mechanical high shear disintegration and homogenization to incorporate them into aerogel matrix as a precursor material (Mikkonen et al., 2013). Nanocelluloses are available in two forms namely: (i) cellulose nanofibre (CNF) and (ii) cellulose nanocrystals (CNC). These two forms of cellulose possesses some unique characteristics like high compressive strength, tunable surface chemistry and high SSA. Moreover, it is considered as the most utilized biopolymer due to those aforesaid unique characteristics which accounts for controlled interactions with biological materials, other polymers, small molecules and other nanoparticles. Morphology of CNF based aerogel is more rice-shaped however, CNC based aerogel displays spherical morphology. Moreover, the apperance of aerogel is affected by the shape of nanocellulose materials. Zhang et al. (2018) reported that combination of CNF and CNC in aerogels gives better performance than aerogel made purely by CNF and CNC. Zheng et al. (2017) reported that CNC based aerogel exhibit good mechanical properties and compressive modulus 6 times higher than the pure cellulose based aerogel. Mahfoudhi and Boufi (2017) reported that cellulose, nanocellulose, CNFs are potentially used for purification of water and Gopakumar et al. (2020) reported that heavy metal ions (Pd^{2+}, Hg^{2+} etc.) can be adsorbed from industrial waste water by cellulose based aerogels thus, recycling of water is possible. de Oliveira, Bruni, El Halal, et al. (2019) reported that CNC aerogels developed from rice and oat husks with nanocrystals diameter ranges from 16.0 to 28.8 nm and water absorption capacity ranges from 264.2 % to 402.8 %, can be used as moisture absorber in food packaging applications.

2.5.1.2 *Starch based aerogel*

Starch have gained imporatnce as a precursor material of aerogel (**Table 2.1**) manufacturing due to their extraordinary characteristics (non-toxic, non-allergenic, most abundant, cheap, GRAS: generally recognized as safe) and diverese range of applications (Ubeyitogullari & Ciftci, 2017; Zhu, 2019). These quality traits of starch made it suitable for developing attractive aerogels with nutrition providing capability and other food-related uses (packaging) (Zhao et al., 2018). Corn starch is one of the widely used starch among all starch. Corn starch-based aerogel have used in different areas according to their quality characteristics (**Table 2.2**). Starch granules size is within micrometer range (1-100 μm). Amylose (smaller and linear) and amylopectin (larger and branched) are the main constituents of starch which differs one starch from other and also regulates the charcteristics of starch subjected to different processing condition. During cooking with water, gelatinization of starch (starch granules swells, then collapse and finally it losses its crystalline structure) takes place. However, when it is subjected

to cooling, retrogradation (starch granules re-associate and re-oredered themselves and develops a degree of crystallinity) takes place (Zhu, 2019). Generally, two steps are followed to make starch based aerogels: (i) hydrogel formation (starch-based) and (ii) drying. Source of starch and amylose-amylopectin ratio plays an important role in end properties of aerogel (Wang et al., 2019). Gel is formed in the process of cooling therefore, amylose content plays an important role in crystal neuclei formation during retrogradation. Hence, the higher the amylose content the faster the retrogradation. Hydrogel is formed only after completion of nucleation, propagation and maturation (Zheng et al., 2020). Moreover, one major concern in aerogel manufacturing is to maintain the porous structure of hydrogel and avoid shrinkage during drying process (Garćia-González, Uy, et al., 2012). Druel et al. (2017) reported a study on starch based aerogels with varying amylose content and concluded that SSA is increased and resistance to shrinkgae is decreased with the increasing amylose content however, due to heterogenous sturcture pur amylose did not able to sustain drying pressure thus, did not form aerogel. Moreover, increasing retrogradation time significantly decrease SSA. Kenar et al. (2014) reported starch based aerogels with SSA 313-362 m^2/g and density 120-185 kg/m^3 through controlled retrogradation. However, starch based aerogels lacks hardness and therfore, crosslinking agent might be reinforced with starch to provide structural stability and pre-requsite properties (Ubeyitogullari, Brahma, Rose, & Ciftci, 2018). Ubeyitogullari and Ciftci (2016) have developed edible aerogels from wheat starch which possess densities 50 - 290 kg/m^3, SSA 52.6-59.7 m^2/g, pore size 20 nm and thermal stability upto 280 °C. Starch based aerogels have diverese range of applications like encapsulation and controlled release of bioactive compounds including food ingredients and drugs, carriers of high value compounds (quercetin) due to their capability to improve solubility and bioavailability of those compounds (Lovskaya et al., 2015; Franco et al., 2018; De Marco et al., 2019), food packaging (lignocellulose naofibrils incorporated in corn starch aerogel to provide water absorption; Ago, Ferrer, and Rojas, 2016), antibacterial and antioxidants in active packaging, providing barrier to external conditions (De Souza et al., 2014; Zheng et al., 2020).

2.5.1.3 *β-Glucan based aerogel*

β-Glucan is a polysaccharide which consists of β-D-glucopyranosyl units connected by β(1-4) and β(1-3) glycosidic linkages. Oat and barley grains are the major sources of β-glucan typically, it is available at a concentration of 3-7 % of grain weight. Especially, due to its high viscosity, it has gained more attention regarding its health promoting activities (reducing postprandiaal serum glucose level and plasma cholestrol). Moreover, β-glucan forms hydrogel

which is 4.5 times stronger than corn starch gel (Comin et al., 2012b). However, due to presence of long chain linkages and higher molecular weight (MW), they exhibit less mobility thus, prevents gel formation. Lazaridou et al. (2003) reported that MW ranges from 35 to 140 kDa would form gel however, samples having MW 250 kDa did not form gel. This may be amalgamated to less molecular interactions due to decreased mobility of longer chains. Comin et al. (2012a) reported formation of low MW β-glucan based aerogel (**Table 2.1**) using $SCCO_2$ drying. They have encapsulated flax oil on this aerogel and suggested applications of those aerogels as a delivery vehicle of functional compounds (flax oil: bioactive lipid rich in ω-3 fatty acids, other bioactive compounds, nutraceuticals etc.). Moreover, in another study, Comin et al. (2012b) reported formation of low MW β-glucan based aerogels using $SCCO_2$ drying. They formed aerogels with density 200 kg/m^3 and SSA 166 m^2/g at 5 % concentration of β-glucan. They have suggested that β-glucan aerogels have huge potential to act as delivery veichel of functional as well as nutraceutical compound as they are edible, renewable, biodegradable, and biocompatible. Nevertheless, Comin et al. (2015) reported that, as a flax lignan carrier β-glucan based aerogels can be potentially used to promote human health.

2.5.1.4 *Alginate based aerogel*

Alginate is a linear structured (consists of α-L-guluronic acid and 1,4-linked-β-D-mannuronic acid) polydisperse polysaccharide. Generally, alginate aerogels are available in beads (<1000 μm) and spherical form (dos Santos et al., 2020). After solvent exchange alginate alcogels have retained the structure thus, during $SCCO_2$ drying structure collapse is avoided (Baldino, Cardea, Scognamiglio, and Reverchon, 2019). Pure alginate aerogel (**Table 2.1**) possesses superior qualities (pore size: 1081 nm, pososity: 65.60 %, density: 615.8 kg/m^3, SSA: 16.76 m^2/g and water solubility: 44.61 %) than pure starch aerogels (Martins et al., 2015; Chen and Zhang, 2019; Selvasekaran and Chidambaram, 2021). However, low mechanical performance is one major drawback of alginate based aerogels. Hou et al. (2020) reported that as a novel approach covalent and ionic crosslinking in alginate based aerogel could results in high strength aerogels with double catalytic performance. Alginate based aerogels can be used in various food applications (packaging, bioactive carriers, mineral ions carrier) after improving the physicochemical and mechanical characteristics through hybridization approach (Selvasekaran and Chidambaram, 2021).

2.5.1.5 *Pectin based aerogel*

Pectin is one of the major structural polysaccharides. Ripe fruits, by-products of fruit juices, sunflower oil etc. are some common sources of pectin. Few hundred to thousand galacturonic

acid monomers are contained in pectin which are connected by α-(1→4)-glycosidic bond and undergoes methyl esterification. The degree of esterification (DE) classifies pectin in two groups: (i) high-methoxyl pectin (DE>50 %) and (ii) low-methoxyl pectin (DE<50 %) (Gawkowska, Cybulska, and Zdunek, 2018). In the presence of acids and sugars high-methoxyl pectin forms stable gel, the mechanism involves in gelation of high-methoxyl pectin is partial dehydration of pectin molecules. Whereas, in the presence of divalent ions low-methoxyl pectin forms gel, involves mechanism of egg-box model (Zhang, Zhang, and Yuan, 2020). Nevertheless, the physical stability and SSA of aerogel (**Table 2.1**) depends on the source of pectin and gelation mechanism. It is worth mentioning that amidation of galacturonic acid improves gelation of low-methoxyl pectin which reduces the use of crosslinkers, as a result notable increase in food grade aerogel production is observed (De Cicco et al., 2016; Selvasekaran and Chidambaram, 2021). Veronovski et al. (2014) reported aerogel production using amidated low-methoxy pectin from apple fruit and citrus fruit with minimal use of crosslinker $CaCl_2$. Groult and Budtova (2018) produced pectin based aerogels using ethanol and acetone individually as exchanger solvent and revealed density of 110 and 65 kg/m^3, SSA of 570 and 630 m^2/g respectively for ethanol and acetone. The changes may be attributed to lesser miscibilty of ethanol with CO_2 than acetone. Moreover, enhancement of hydrogel firmness and declination in volume shrinkage rate of pectin aerogels is due to sugar content of pectin (Kastner, Einhorn-Stoll, and Senge, 2012). Pectin based aerogels can be used as a carrier of functional compounds in food industry and edible aerogels made of pectin could be directly consumed as it provides numerous health benefits (reduce blood cholestrol, adsorb toxic cations like Pb^{2+}, Hg^{2+}, etc.).

2.5.1.6 *Carrageenan based aerogel*

Carrageenan is a linear sulphated polysaccharide which is comosed of alternative units of 3,6-anhydro-α-D-galactose and β-D-galactose units, connected by α-(1,3) and β-(1,4) glycosidic bonds. Mohammad Alnaief, Obaidat, and Mashaqbeh (2018) revealed that, as the concentration of k-carrangeenan increased, network density of aerogels increases, textural properties of aerogels improve and yield larger particle size aerogel. However, in contrary, Manzocco et al. (2017) reported decrease in network density with the increase in concentration of k-carrageenan. The first k-carrageenan based aerogel with dual pore structure was synthesised by Ganesan and Ratke (2014). They reported that without using crosslinker stable aerogels can not be derived as lower concentration of k-carrageenan forms weakly bound porous network due to less intercrosslinking junctions of fibers. However, higher concentration (4 %) of k-

carrangeenan is avoided as the solution become highly viscous and handling is not easy. As a best crosslinker a monovalent cation (k+) was found. The major drawback exhibited by k-carrageenan based aerogels is higher volume shrinkage due to increase of repulsive force and ionic strength as a result of hydration of sulphated functional group during hydrogel formation and due to reduction of repulsive force during solvent exchange (Ganesan and Ratke, 2014; Selvasekaran and Chidambaram, 2021). The gelation of k-carrageenan based aerogel takes place in the presence of ionic liquids (Kadokawa, 2011). Agostinho et al. (2020) reported k-carrageenan based aerogels from supercritically dried ionogels. It possess similar characteristics (softness, color, SSA, opaquness, macropores and mesopores etc.) as potassium salt crosslinkers based aerogels. However, it possess less volume shrinkage than those potassium salt crosslinker based aerogels. Plazzotta, Calligaris, and Manzocco (2019) reported lettuce homogenate and k-carrageenan based aerogel having porosity 90 % and mean pore size 100 μm. Carrageenan based aerogel can be used to make oleogel and exploited for novel food application (nutrients, aroma compounds, additives carrier and active packaging) (Manzocco et al., 2017).

Table 2.1 Polysaccharide based aerogel, their characteristics, and application

Polysaccharide precursor	Gelation method	Chemical cross-linker	Drying method	Properties	Potential application
Nanofibrillated cellulose	Osmotic concentration using dextran solution	-	Spray-freeze drying	SSA:80-100 m^2/g, BD:0.012-0.033g/cm^3, D_P:10-100 nm, ε:98-99 %	Superinsulating packaging material (Low thermal conductivity of 0.018 W/m-K)
Cellulose nanocrystals (rice husk)	Thermal gelation	-	Freeze drying	-	Water absorber in food packaging (water absorption capacity of 357.5 %)
Cellulose nanocrystals (oat husk)					Water absorber in food packaging (water absorption capacity of 402.8 %)
Starch (corn)	Emulsion gelation	-	$SCCO_2$ drying	SSA:93 m^2/g, V_P:0.69 cm^3/g, D_P:24-25 nm, ε:87.7, P_M:1.2 µm	Loading and controlled release of bioactive compounds
Starch (wheat)	Gelatinization and retrogradation	-	$SCCO_2$ drying	SSA:52.6-59.7 m^2/g, V_P:0.09-0.27 cm^3/g, BD:0.05-0.29g/cm^3, D_P:20 nm	Bioactive carriers and fillers in food preparations
Starch (corn)	Emulsion gelation	-	$SCCO_2$ drying	SSA:34-120 m^2/g, V_P:0.12-0.36 cm^3/g, P_M:215-1226 µm	Chemical compounds carrier
Starch (wheat)	Gelatinization and retrogradation	Sodium metaphosphate	$SCCO_2$ drying	SSA:48.9 m^2/g, BD:0.13g/cm^3, V_P:0.19 cm^3/g, D_P:16.5 nm, ε:91.7 %	Promising functional food ingredient with high resistant starch content, even after cooking also
β-Glucan	Thermal gelation	-	Air drying, freeze drying, $SCCO_2$ drying	SSA:166 m^2/g, BD:0.20g/cm^3	Delivery vehicle for nutraceuticals
Alginate	Sol-gel method	Calcium chloride (450 mmol)	Freeze drying	BD:0.6158 g/mL, D_P:1081 nm, ε:65.60 %	-

Pectin (apple fruit)-1 % (w/w)	Ionotropic gelation	Calcium chloride	$SCCO_2$ drying	SSA:515 m^2/g, V_P:0.95 cm^3/g, D_P:8.7 nm	Carry and release functional compounds on the target area
Pectin (apple fruit)-2 % (w/w)				SSA:213 m^2/g, V_P:0.339 cm^3/g, D_P:7.5 nm	
Pectin (citrus fruit)-1 % (w/w)				SSA:143 m^2/g, V_P:0.214 cm^3/g, D_P:7.2 nm	
Pectin (citrus fruit)-2 % (w/w)				SSA:248 m^2/g, V_P:0.39 cm^3/g, D_P:7.4 nm	
k-carrageenan	Emulsion gelation	Potassium chloride, Potassium carbonate, Aluminum chloride, Potassium Iodide	$SCCO_2$ drying	SSA:34-174 m^2/g, V_P:0.10-0.54 cm^3/g, BD:0.06-0.50g/cm^3, D_P:7.4-16.5 nm, P_M:6.67-189.91 μm	Functional compound delivery system
k-carrageenan	Inotropic gelation	Potassium chloride	$SCCO_2$ drying	V_P:0.308 cm^3/g, ε:94.3 %	Edible (food grade) oleogel production
			Freeze drying	V_P:0.004 cm^3/g, ε:95.9 %	
k-carrageenan	Dissolution into ionic liquids using cross-linkers	Potassium chloride, Potassium thiocyanate	$SCCO_2$ drying	SSA:123-221 m^2/g, V_P:0.32-0.52 cm^3/g	Bioactive compound delivery systems

SSA=Specific surface area; V_P=Pore volume; D_P= Average pore diameter; BD=Bulk density; P_M=Mean particle size; ε=Porosity; $SCCO_2$: Supercritical carbon dioxide; '-': not available. [Source: Jim´enez-Saelices et al., (2017); de Oliveira, Bruni, Fabra, et al., (2019); Goimil et al., (2017); Ubeyitogullari and Ciftci, (2016); García-Gonz´alez, Uy, et al., (2012); Ubeyitogullari et al., (2018); Comin et al., (2012b); Chen & Zhang, (2019); Veronovski et al., (2014); Alnaief et al., (2018); Plazzotta et al., (2019); Agostinho et al., (2020)]

Table 2.2 Corn starch based aerogel, their characteristics, and application

Starch concentration (wt %)	Amylose content (%)	Gel temperature (°C)	Drying method	Total shrinkage (%)	Density (g/cm^3)	Porosity (%)	Specific surface area (m^2/g)	Water absorption capacity (%)	Application
10	70	90	Supercritical CO_2 drying	48	0.198	95		200	Loading and release of active compounds, absorbents
		110		43	0.145	93			
15		90		47	0.251	89		≈ 230	
		110		48	0.201	90			
8	80	95 to 140	Supercritical CO_2 drying	≈ 36	0.140	-	254	-	Thermal super-insulating material
15	-	110	Supercritical CO_2 drying	-	-	-	80	-	Active packaging material loaded with quercetin
10	29.7	90	Freeze drying	-	-	-	-	-	Phenolic compound carrier material
					0.03			≈ 683	Active packaging material loaded with phenolic compounds
15	-	75	Supercritical CO_2 drying	-	-	-	64.320	-	β-carotene loaded aerogel
									β-carotene loaded aerogel

≈ 17	31.2	90	Freeze dryer	-	-	-	-	-	β-carotene loaded aerogel
15	-	75	Supercritical CO_2 drying	-	-	-	63.621	-	Polyphenols impregnated aerogel
8	1	90, 130-140	Supercritical CO_2 drying	≈ 38-39	≈ 0.35-0.60	≈ 56-75	≈ 7-20	-	-
11				≈ 28-38	≈ 0.3-0.4	≈ 72-79	≈ 30-90		
8			Freeze drying	-	≈ 0.10	≈ 93	≈ 5-6		
11					≈ 0.15	≈ 90	≈ 4		

'-': not available. [Source: Dogenski et al., (2020); Druel et al., (2017); Franco et al., (2018); Fonseca et al., (2020); Fonseca et al., (2021); Dias et al., (2022); Hatami et al., (2024); Zhang et al., (2023); Araujo et al., (2023); Zou and Budtova, (2021)]

2.5.2 *Protein based aerogel*

Protein is an important compound which helps to build and repare body tissue, provide energy and maintain metabolic reactions etc. Therefore, protein based aerogel (**Table 2.3**) as a distinct way of protein delivery could offer diverse range of opportunities for application in foods. Whey, egg, and sodium caseinate proteins are most reliable proteins suitable for consumption.

2.5.2.1 *Whey protein based aerogel*

In this context, whey protein filtered from cheese whey could be a good source of protein as well as it will serve as a precursor material of functional foods. However, the use of whey protein is restricted due to its bitter taste caused by peptides present within the whey protein matrix. Moreover, masking agents (sodium glutamate, monosodium glutamate etc.) can be used to ovecome this problem (Leksrisompong et al., 2012). The $SCCO_2$ dried whey protein aerogels provide higher porous surfce and less aggregation of particle than freeze dried whey protein aerogels. Plazzotta, Calligaris, & Manzocco (2020) reported densities of 21 kg/m^3 and 70 kg/m^3 for $SCCO_2$ and freeze dried whey protein aerogels respectively which supports the previous argument. Betz et al. (2012) reported that during the production of aerogels, a crosslinked gel structure is formed due to irreversible aggregation of thermally denatured whey proteins. Chen, Wang, and Schiraldi (2013) reported that even though the concentration of whey protein is increased in its pure form, provide brittle structure and poor mechanical strength. Chen, Wang, and Schiraldi (2013) reported crossinking of Na^+ ions with whey protein isolate produces aerogels with better mechanical strength. Moreover, co-polymerization increases viscosity however, it possess imperfect structure due to air bubbles trapping into the solution.

2.5.2.2 *Egg white protein based aerogel*

Thermal denaturation of egg white protein forms gel easily which exhibit rapid increase in aerogel fabrication. According to Selmer et al. (2019), emulsion gelation and $SCCO_2$ drying forms egg white protein aerogels with bulk density of 179 kg/m^3, SSA of 232 m^2/g, mean pore diameter of 41.7 nm, mean particle size of 32.7 nm and pore volume of 2.28 cm^3/g. The ionic strength and pH of egg white protein hydrogel regulates end properties of aerogels (Kleemann et al., 2018). The pH of hydrogel close to isoelectric point exhibit less SSA than the pH beyond the isoelectric point. Selmer et al. (2015) reported that at pH 4.6 (nearer to isoelectric point) of hydrogel, aerogel possess SSA of 16 m^2/g whereas, at pH 2 it yields SSA of 380 m^2/g. Moreover, pH beyond isoelectric point (2, 3.5, 9 and 11.5) exhibit homogeneous and dense

structure and this may be due to induction of strong repulsive forces between protein molecules at high and low pH which ultimately slows down the aggregation process during gel network formation. Whereas, at isoelectric point, protein molecules lacks repulsive force which leads to fast aggregation. Moreover, protein subunits having partially positive and negative charges aggregated with each other and forms coarseand heterogeneous network (Kleemann et al., 2018). Selmer et al. (2015) also reported that addition of sodium chloride salt with an increasing concentration results in aerogels with higher number of pores, coarse structure and low SSA which may be attributed to fast aggregation due to lack of repulsive forces (intermolecular) as a consequence of shielding of charges of protein molecules.

Table 2.3 Protein based aerogel, their characteristics, and application

Protein precursor	Gelation method	Drying method	Properties	Potential application
Whey protein isolate (washing media-deionized water)	Emulsion gelation	$SCCO_2$ drying	SSA:354 m^2/g, V_P:1.55 cm^3/g, D_P:14.0 nm, BD:241 g/cm^3, P_M:66.6 µm	Carrier material for sensitive oils and food additives
Whey protein isolate (washing media-10mM $CaCl_2$)			SSA:154 m^2/g, V_P:0.33 cm^3/g, D_P:7.1 nm, P_M:47.3 µm	
Egg white protein			SSA:232 m^2/g, V_P:2.28 cm^3/g, D_P:41.7 nm, BD:179 g/cm^3, P_M:32.7 µm	
Sodium Caseinate			SSA:48 m^2/g, V_P:0.28 cm^3/g, D_P:13.4 nm, BD:443 g/cm^3, P_M:40.9 µm	
Whey protein isolate	Heat set	$SCCO_2$ drying	SSA:390-422 m^2/g, V_P:1.27-1.69 cm^3/g, D_P:9.2-14.0 nm	Microencapsulation purposes in food and targeted release of encapsulated compounds
Egg white protein			SSA:220-378 m^2/g, V_P:1.56-2.79 cm^3/g, D_P:13.8-17.4 nm	
Sodium Caseinate	Enzymatic crosslinking		SSA:42 m^2/g, V_P:0.24 cm^3/g, D_P:9.2 nm	
Soy protein	Heat set	$SCCO_2$ drying	SSA:384-478 m^2/g, V_P:0.12-0.15 cm^3/g; 1.72-2.29 cm^3/g; 1.41-2.72 cm^3/g, BD:0.19-0.25 g/cm^3, P_M:4-50 µm	Renewable natural superinsulators
Silk fibroin	Heat set	$SCCO_2$ drying	SSA:424 m^2/g, D_P:5-130 nm, BD:0.058 g/cm^3	Functional compounds delivery systems, even for an extended period of time

SSA=Specific surface area; V_P=Pore volume; D_P= Average pore diameter; BD=Bulk density; P_M=Mean particle size; $SCCO_2$: Supercritical carbon dioxide. [Source: Selmer et al., (2019); Kleemann et al., (2020); Amaral-Labat et al., (2012); Marin et al., (2014)]

2.5.2.3 *Sodium caseinate aerogel*

Selmer et al. (2019) produced sodium caseinate aerogels with mean particle size of 40.9 µm, bulk density of 443 kg/m^3, pore volume of 0.28 cm^3/g and SSA of 48 m^2/g. Kleeman et al. (2018) reported enzymatic cross-linking during hydrogel formation process. TGase as a cross-linker is used with sodium caseinate, as the protein concentration is increased, stiffness and mechanical properties are also increased gradually due to proper forming of covalent bonds between protein molecules. The major drawback is low SSA (approximately ½ to ¼ th of egg white and whey protein aerogels), attributed to fast aggregation and random cross-linking of protein molecules. Moreover, casein molecules covalent cross-linking hinders aerogel disintegration in aqueous medium (Kleemann et al., 2020). Sodium caseinate aerogels can be applied in the field of functional compound delivery systems due to their good controlled release property. Kleemann et al. (2020) reported controlled release of encapsulated fish oil from sodium caseinate aerogel matrix. As an encapsulation material and carrier material these can be used. Moreover, Selmer et al. (2019) reported sodium caseinate aerogel as a carrier material of fish oil with free flowing ability and without leakage upto 12 weeks of storage.

2.5.3 *Seed mucilage based aerogel*

Mucilage is similar to common gums, possess good functional characteristics and water holding capacity, can be used as a thickener and stabilizer. Seed mucilage consists of mixture of small amount of proteins and various polysaccharides. However, depending upon the source of seed, mucilage varies. Various seed mucilage based aerogel (**Table 2.4**) are discussed below.

2.5.3.1 *Flaxseed mucilage based aerogel*

Flaxseed mucilage contributes upto 10 % of seed weight and found in outermost layer (mucous epidermis) of flaxseed coat. Mucilage composed of two heterogenous polysaccharides: (i) arabinoxylan (75 %, neutral) and (ii) rhamnogalacturanan (25 %, acidic). Thermo-reverssible cold-set weak gel can be formed using flax mucilage (Comin et al., 2015). Flax mucilage based aerogels was first developed by Comin et al. (2015) and they reported aerogels with end properties like SSA of 201.1 m^2/g, low density of 160 kg/m^3, average pore diameter of 25.2 Å and pore volume of 0.82 cm^3/g. Below 10 % (w/v) concentration of flax mucilage, it is found to be difficult to retain the shape of hydrogel, considered as a major drawback. Moreover, weak hydrogel which results in deformed morphology (aerogel) was formed. Flax mucilaged based aerogel can be used as a delivery vehicle for bioactive compounds (Comin et al., 2015).

2.5.3.2 *Camelina seed mucilage based aerogel*

Camelina sativa L. Crantz which contains 28 to 40 % oil (mainly ω-3-fatty acids), excretes camelina seed mucilage. Due to its extraordinary swelling kinetics and water absorption capacity it forms good hydrogel network in the presence of water. With nanoporous structure and high SSA, camelina mucilage aerogel as a novel food grade aerogel was first developed by Ubeyitogullari and Ciftci (2020). Camelina mucilage at a concentration lower than 10 % (w/w) lacks the ability to maintain the shape of hydrogel. Ubeyitogullari and Ciftci (2020) reported that, mucilage concentrate and powder derived aerogels exhibit excellent properties like density of 80 and 50 kg/m^3, SSA of 240 and 229 m^2/g, pore size of 6.0 and 5.6 nm, pore volume of 0.32 and 0.28 cm^3/g and porosity of 91 and 94 % respectively. Nevertheless, the cylindrical shape of aerogels with minimum shrinkage was retained by both the aerogels. Mucilage aerogel used in various food application due to their ability to increase bioavailability of the water-insoluble bioactive compounds. As a thickner and stabilizer these aerogels can be used in different food applications (Ubeyitogullari and Ciftci, 2020).

2.5.3.3 *Balangu seed mucilage aerogel*

Balangu (*Lallemantia royleana*) belongs to *Labiatae* family. Carbohydrates, protein, oil and fiber is found in balangu seed. In Iranian food industry balangu seeds are used as food additive and gelling agent. Balangu seeds possess good health benefits by preventing nervous diseases, inflammation, high blood pressure, sore throats, abscesses and respiratory problems. Balangu seed mucilage (BSM) is a long-chain polysaccharide having high molecular weight (3.65×10^6 g/mol). When BSM dissolves in water, it forms turbid, tasteless, and sticky liquid. Balangu seed based aerogel was first produced by Falahati and Ghoreishi (2019) and they reported balangu seed based aerogel with SSA of 95.74 m^2/g and pore volume 0.368 cm^3/g. Immense structural shrinkage was observed during solvent exchange and $SCCO_2$ drying however, highly porous structure was retained. Falahati and Ghoreishi (2019) reported use of balangu seed mucilage aerogels as a prcursor of drug (paracetamol) delivery applications due to its controlled release behaviour. Therefore, balangu seed mucilage aerogels can also be used as functional compound delivery system in food industries.

Table 2.4 Mucilage based aerogel, their characteristics, and application

Mucilage precursor	Gelation method	Drying method	Properties	Potential application
Flax mucilage (10 % w/w)	Sol-gel	SC-CO_2 drying	SSA:201.1 m^2/g, V_P:0.82 cm^3/g, D_P:25.2 Å, D:0.16 g/cm^3	Delivery vehicle for nutraceuticals, including Flax lignan, secoisolariciresinol diglucoside
Balangu seed mucilage (0.04 g/ml)	Ethanol induced gelation	SC-CO_2 drying	SSA:95.74 m^2/g, V_P:0.368 cm^3/g, P_S:1.29 nm	Functional compound delivery system
Camelina seed mucilage concentrate (10% w/ w)	Sol-gel	SC-CO_2 drying	SSA:228.7 m^2/g, V_P:0.28 cm^3/g, P_S:5.6 nm, D:0.05 g/cm^3, ε:94.3%	Enhance the bioavailability of water-insoluble bioactives in food formulation, stabilizing and thickening of different food formulations
Camelina seed mucilage powder (10% w/ w)			SSA:239.5 m^2/g, V_P:0.32 cm^3/g, P_S:6.0 nm, D:0.08 g/cm^3, ε:91.0%	

SSA=Specific surface area; V_P=Pore volume; D_P= Pore diameter; D=Density; P_S=Pore size; ε=Porosity; $SCCO_2$: Supercritical carbon dioxide. [Source: Comin et al., (2015); Falahati and Ghoreishi, (2019); Ubeyitogullari and Ciftci, (2020)

2.5.4 *Hybrid or composite aerogel*

Hybrid or composite aerogel (**Fig. 2.1; Table 2.5**) are those which have developed by using more than one precursor material (it may be same kind of material: polysaccharide-polysaccharide or different kind of material: polysaccharide-protein or a cross-linker). Composite aerogel have developed to overcome some specific problems like, improvement of mechanical properties, maintaining porous structure of hydrogel network, avoid volume shrinkage etc. Hybridization is done also to produce bioactive packaging structures for controlled release of bioactive compounds into the food system (de Oliveira, Bruni, El Halal, et al., 2019). Arboleda et al. (2013) produced soy protein-nanocellulose composite aerogel. Practically, it is very difficult to produce aerogel using only soy protein (SP) as precursor material as they are brittle and having less mechanical strength. However, utilization of soy protein in aerogel formation can not be neglected due to its diverse range of use such as functional compound delivery, reducing oxidative stress, in adhesieves, emulsions, etc. To overcome those aforesaid problems nanofibrillar cellulose (NFC) is added with SP. The authors have revealed that addition of NFC enhances the mechanical characteristics of aerogel. Low amount of solid content in precursor hydrogels produces low density (111- 115 kg/m^3) composite SP-NFC aerogel. The application of SP-NFC composite aerogel can be as delivery vehicle for functional compounds in food packaging systems (Arboleda et al., 2013).

de Oliveira, Bruni, Fabra, et al. (2019) produced hybrid PVA aerogel reinforced with nanocellulose and cellulose extracted from *Gelidium sesquipedale* seaweed. Pure PVA aerogels releases bioactive compound immediately. Therefore, this study has been conducted to investigate the release of bioactive agar based extract obtained from *Gelidium sesquipedale* seaweed into hydrophobic and hydrophilic food products and how nanocellulose and cellulose addition influences the hydrogel. The authors have revealed that hybrid aerogel has preserved their integrity and exhibit more controlled release. Both the hybrid aerogel possess similar release characteristics however, nanocellulose based hybrid aerogel exhibit grater release values after more prolonged times. This hybrid aerogel can be used for the development of packaging structure based on bioactive compounds.

Nešić et al. (2018) produced pectin-TiO_2 composite aerogels through sol-gel process to store temperature-sensitive foods. These aerogels exhibit thermal conductivity (0.022-0.025 W/m-K) value lower than air (0.024-0.032 W/m-K). Thermal conductivity of pectin based aerogel depends upon density of aerogel which is influenced by process conditons like solvent pH and degree of cross-linking (Groult & Budtova, 2018).

Table 2.5 Hybrid/Composite food aerogel and their potential application

Precursor material	Key findings	Potential application
PVA-Cellulose-YBME PVA-Nanocellulose-YBME	• Cellulose, nanocellulose obtained from yerba-mate *(Illex paraguariensis*) • yerba-mate based extract (YMBE) encapsulated in hybrid aerogels • nanocellulose exhibit rod-like morphology • Cellulose and nanocellulose based hybrid aerogels produced homogeneous structure with porosity, without separation of polymer matrix and exhibited antioxidant activity more than 80 % • Cellulose based aerogel releases more YMBE in hydrophobic foods whereas nanocellulose based aerogel releases more YMBE in hydrophilic foods	Food preservation and active packaging
F2A-HW(S)	• *Arundo donax* waste biomass lignin and hot water extract of *Arundo donax* waste biomass was used for hybrid aerogel formation • Freeze drying method is used • Hybrid aerogels exhibit complete release of extract in hydrophilic media	Bioactive food packaging pads
Soy protein-Nanocellulose	• Soy protein-Nanocellulose composite aerogels have developed using thermal gelation and freeze drying • fibrous and small leaf-like morphological structures were observed • Density was in the range of 0.111–0.115 g/cm^3 • Absorb moisture up to 5 % from humid air (relative humidity 50%) • Mechanical properties and loading capacities improved	Delivery vehicle of functional compounds
Pectin-TiO_2	• Pectin-TiO_2 nanocomposite aerogels are produced through sol-gel process and supercritical drying • tert-butanol and zinc ions induces cross-linking • Mechanical, thermal, and antimicrobial properties improved due to addition of TiO_2 • Hybrid aerogel possess thermal conductivity (0.022 – 0.025 W/m-K) lower than air	Storage of temperature sensitive food Bio- and short life food packages (food delivery package)

PVA-Cellulose-Agar based extract of GS PVA-Nanocellulose-Agar based extract of GS	• *Gelidium sesquipedale* sea weed is used to extract cellulose and nanocellulose • Agar based extract of *Gelidium sesquipedale* sea weed is incorporated into the hybrid aerogel systems • Cellulose and nanocellulose based aerogels maintained their integrity, gradual release of bioactive compound was observed, both of the composite aerogel exhibit similar release characteristics up to 48 h however, in prolonged duration nanocellulose based aerogels led to greater release values	Absorbent pads in fresh meat and fish products due to their high water absorption capacity Active food packaging Release of the bioactive in hydrophobic and hydrophilic food simulant media
Alginate-hyaluronic acid	• Emulsion gelation and supercritical CO_2 technique was used • Particle agglomeration is reduced • Biodegradability is expected to be increased • Particle size ranges between 1 to 5 µm • Mean particle diameter ranges from 33.0-40.0 µm • Density and porosity ranges from 0.035-0.063 g/cm^3 and 97.6-98.7 % respectively	Bioactive delivery systems

PVA: Poly vinyl alcohol; YMBE: Yerba-mate based extract; F2A-HW(S): lignin-hot water extract; TiO_2: Titanium dioxide. [Source: Oliveira et al., (2020); Fontes-Candia et al., (2019); Arboleda et al., (2013); Nešić et al., (2018); Oliveira, Bruni, El Halal, et al., (2019); Athamneh et al., (2019)]

2.5.5 *Functional compound impregnated aerogel*

This is the most widely used form of aerogel (**Table 2.6**), in which the aerogel plays the role of delivery vehicle (or carrier matrix) of functional compounds for food applications. Biopolymer based aerogel possesses excellent end properties like high porosity, high mechanical strength and high SSA. Moreover, an aerogel could be a good carrier and releaser, if it possess high SSA, high porosity and high mechanical strength (Selmer et al., 2015). High SSA is needed for adsorption and the high porosity is needed for capillary condentation of functional ingredients. Incorporation of functional compounds (**Fig. 2.3**) can be done prior to hydrogel formation and after super supercritical drying (Selmer et al., 2019). Generally, supercritical impregnation and wet impregnation are the two effective methods of loading functional compounds into the aerogel matrix. The mixture of supercritical fluid and functional compound is diffused into the pores of aerogel in supercritical impregnation (Lopes et al., 2017). Functional compound's chemical adsorption or functional compound's precipitation upon depressurization leads to impregnation later. However, functional compound's solubility influences the impregnation efficiency (dos Santos et al., 2020). Moreover, supercritical fluid extraction of organic solvent and antisolvent mechanism for solute precipitation is used for further impregnation of functional compounds (Viganó et al., 2020). Functional compound containing solvent brought into contact with produced alcogel for a specific time duration in wet impregnation. Therefore, biodegradable, biocompatible, environment friendly nature of precursor materials along with functional compounds carrying and releasing capability leads to develop functionally active aerogels with diverse range of application in food sector (Selvasekaran and Chidambaram, 2021).

Oliveira et al. (2020) produced yerba-mate cellulose and nanocellulose based bioactive aerogels to deliver yerba-mate based extract (YMBE) as bioactivity exhibitor. The authors have reported that yerba-mate cellulose based aerogel indicates more release of YMBE in hydrophobic foods and yerba-mate nanocellulose based aerogel indicates more release of YMBE in hydrophilic foods. These aerogel could be used in food presevation and active packaging of food.

Franco et al. (2018) reported quercetin encapsulated maize starch aerogel and calcium alginate aerogel production. Supercritical adsorptions were performed at a pressure of 180 bar and temperature of 40 °C and 60 °C. They reported increase in solubility of quercetin with the increase in temperature and pressure and may be attributed to the increase in density of CO_2. Pure quercetin exhibits higher dissolution rate than quercetin loaded on aerogels. Therefore,

controlled release system could be obtained through supercritical adsorption. Quercetin impregnated aerogels can be used in active packaging as quercetin possesses extraordinary antioxidant and antimicrobial properties. Therefore, it preserve the food from deterioration due to lipid oxidation during transportation and storage.

Betz et al. (2012) reported whey protein based aerogel production which can serves as a high value functional compounds carrier. Aqueous solution of whey protein is formed into gel through heating at different pH, then the gel was exploited to combine sol-gel and supercritical drying technologies hence, mechanically stable water-insoluble whey protein aerogel with BET-surface area ranges from 310 to 388 m^2/g is formed. These aerogel can be used as a functional compound (probably having high medicinal value) delivery agent.

De Marco and Reverchon (2017) produced poorly water-soluble vitamins loaded starch aerogel. The $SCCO_2$ adsorption technique is adopted to impregnate vitamins. Basically, the authors have used maize starch as precursor material and vitamin E (α-tocopherol) and vitamin K_3 (menadione) as loading materials. The authors have reported 95-98 % vitamin loading with reference to expected concentration for both vitamins. Dissolution rate of vitamin E and vitamin K_3 in loaded aerogel are 16 and 3.5 times faster than unprocessed vitamins respectively.

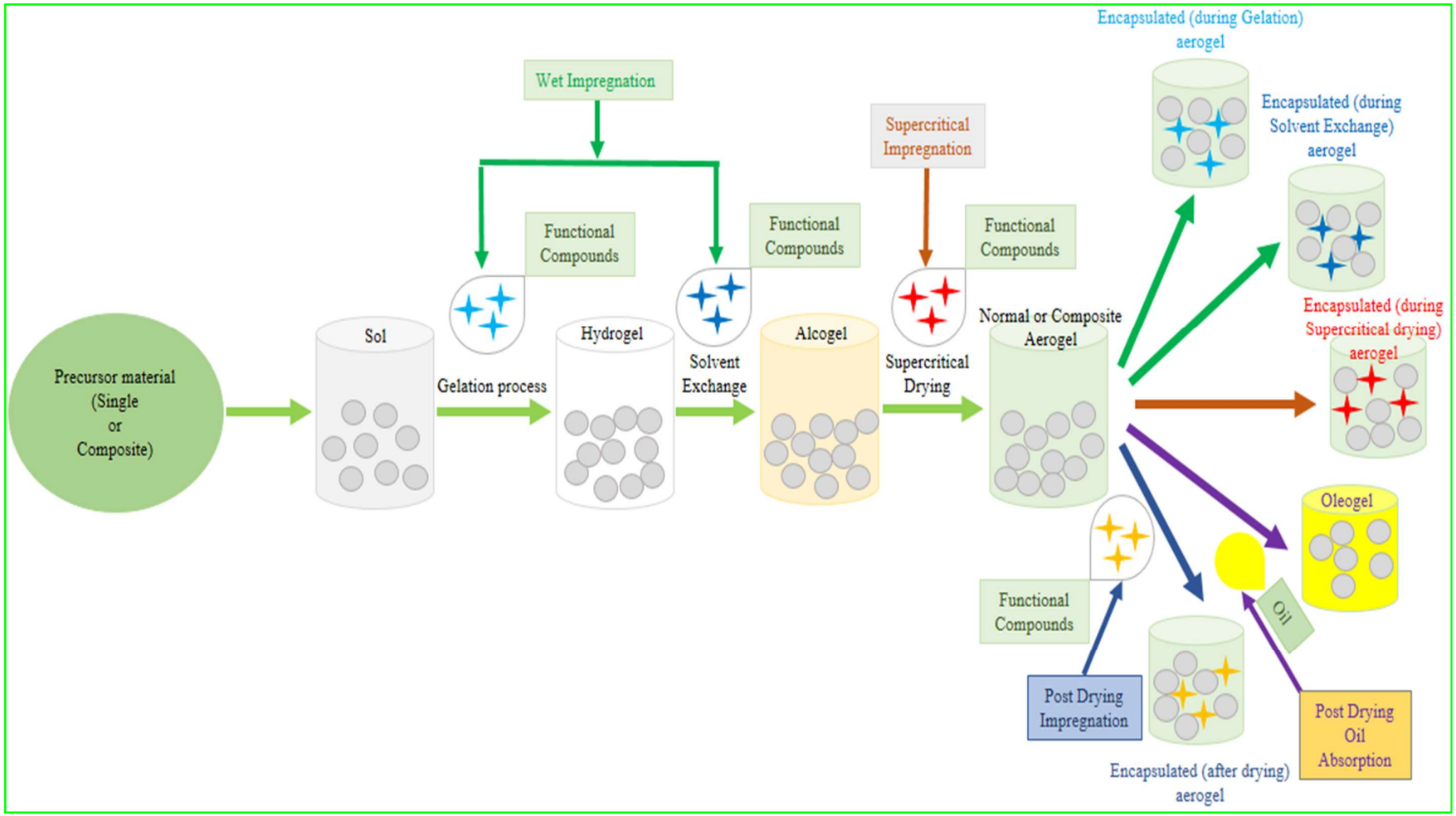

Fig. 2.3 Loading of functional compound at different stages of aerogel preparation

Table 2.6 Functional compound impregnated aerogel

Precursor materials category	Precursor material	Gelation method	Drying method	Loaded compound	Impregnation method	Loading parameters (time & efficiency)
Polysaccharides	Cellulose	Thermal gelation	$SCCO_2$ drying	Phytol	Supercritical impregnation	24 h & 50 wt %
	Cellulose (bacterial)	Thermal gelation	$SCCO_2$ drying	Vitamin C ($_L$-ascorbic acid)	Antisolvent Precipitation with Supercritical Carbon Dioxide	24 h & -
	Alginate	Emulsion-gelation	$SCCO_2$ drying	Extract of passion fruit bagasse (piceatannol and phenolics)	Wet impregnation	24 h & Total loading- 0.62 g/g raw aerogel; piceatannol- 741.85 µg/g raw aerogel; phenolic compounds- 10.77 mg GAE/g raw aerogel
	Alginate	Internal gelation	$SCCO_2$ drying	Phytol	Wet impregnation	3 days & 18.9 %
					Supercritical impregnation	24 h & 22.1 %
				Clinacanthus nutans extract	Wet impregnation	3 days & 18.5 %
					Supercritical impregnation	24 h & 12.7 %
	Sodium alginate	Sol-gel	$SCCO_2$ drying	Resveratol	Wet impregnation	16 h & 6.7-77.1 %
	Alginate	Sol-gel	$SCCO_2$ drying	Vitamin K_3 (2-methyl-1, 4-naphthquinone) Vitamin D_3 (Cholecalciferol)	Supercritical impregnation	24 h & -

	Alginate	Sol-gel	$SCCO_2$ drying	Vitamin D_3 (Cholecalciferol)	High pressure impregnation (employed with both supercritical and liquid carbon dioxide)	24 h & -
	Calcium alginate	Gelatinization and retrogradation	$SCCO_2$ drying	Quercetin	supercritical CO_2 adsorption	24 h & -
	Starch (maize) Starch (potato)	Gelatinization and retrogradation	Integration of gelatinization, retrogradation, and drying (one-pot concept)	Green coffee oil	One-pot impregnation	6-24 h & 39 %
Polysaccharides	Starch (corn)	Gelatinization and retrogradation	$SCCO_2$ drying	Vitamin E (α-tocopherol)	Supercritical impregnation	24 h & -
	Starch (maize)	Gelatinization and retrogradation	$SCCO_2$ drying	Vitamin E (α-tocopherol) Vitamin K_3 (Menadione)	supercritical CO_2 adsorption	24 h & 19.99 % 24 h & 8.76 %
	β-Glucan (barley)	Sol-gel	$SCCO_2$ drying	Flax oil	Supercritical impregnation (using $SCCO_2$ fluid) before, during and after $SCCO_2$ drying	4-24 h & 47.79-60.96 %
		Thermal gelation	$SCCO_2$ drying	BeneFlax (flax lignan concentrate)	Prior to gelation and after gelation	1 h & 34.6-36.5
	Pectin (apple fruit) Pectin (citrus fruit)	Ionotropic gelation	$SCCO_2$ drying	Vitamin B_3 (Nicotinic acid)	Wet impregnation (during sol-gel process)	- & 25 % - & 37 %

	k-Carrageenan	Sol-gel	$SCCO_2$ drying	Sunflower oil	Oil absorption (after completion of aerogel formation)	Until immersion of aerogel template & 80 %
	k-Carrageenan	Sol-gel	Freeze drying	Sunflower oil	Oil absorption (after completion of aerogel formation)	Until immersion of aerogel template & 97 %
	k-Carrageenan	Sol-gel (lettuce homogenate as water phase)	$SCCO_2$ drying	Sunflower oil	Oil absorption (after completion of aerogel formation)	Until immersion of aerogel template & 94.0 %
			Freeze drying			Until immersion of aerogel template & 94.7 %
Protein	Whey protein	Cold set gel	Freeze drying	Fish oil	Immersion of the aerogel into the solution containing equal volume ratio of hexane – fish oil	3 h & 71.7 %
	Whey protein isolate	Heat set gel	$SCCO_2$ drying	Fish oil	Supercritical impregnation	72 h & 33.1–51.1 g fish oil/g aerogel
Protein	Egg white protein	Heat set gel	$SCCO_2$ drying	Fish oil	Supercritical impregnation	72 h & 44.3-63.6 g fish oil/g aerogel
	Sodium caseinate					72 h & 16.6 g fish oil/g aerogel
	Whey protein isolate	Heat set gel	Freeze drying	Sunflower oil	Oil dispersion	16 min (whole process) & 69.3 (g oil/100 g aerogel)
			$SCCO_2$ drying			16 min (whole process) & 84.8 (g oil/100 g aerogel)
	Whey protein isolate	Emulsion gelation	$SCCO_2$ drying	Fish oil	Static supercritical CO_2 impregnation	48 h & 0.74 g fish oil/g aerogel

	Egg white protein Sodium caseinate					48 h & 0.74 g fish oil/g aerogel 16 h & 0.12 g fish oil/g aerogel
Mucilage	Flaxseed mucilage	Thermal gelation	$SCCO_2$ drying	BeneFlax (flax lignan concentrate)	Prior to gelation and after gelation (immersion of hydrogel into solution containing Beneflax+ 70% ethanol)	1 h & 33.2-43.0 %
Composite / Hybrid	Gum tragacanth + PVA	Freeze-thaw method	$SCCO_2$ drying	Silymarin	Vacuum impregnation	165 min (whole process) & 45.57 %
	Alginate + pectin	Sol-gel	Freeze drying	Proanthocyanidins	Wet impregnation (during sol-gel process)	24 h & 15.91 %

$SCCO_2$: Supercritical carbon dioxide; PVA: Poly vinyl alcohol; GAE: Gallic acid equivalent; h: hour; '-': not available. [Source: Lopes et al., (2017); Haimer et al., (2010); Viganó et al., (2020); Mustapa et al., (2016); dos Santos et al., (2020); Pantić et al., (2016); Pantić, Kotnik, et al., (2016); Franco et al., (2018); Villegas et al., (2019); De Marco et al., (2019); De Marco and Reverchon, (2017); Comin et al., (2012a); Comin et al., (2015); Veronovski et al., (2014); Manzocco et al., (2017); Plazzotta et al., (2019); Plazzotta et al., (2019); Ahmadi, Madadlou, and Saboury, (2016); Kleemann et al., (2020); Plazzotta et al., (2020); Selmer et al., (2019); Comin et al., (2015); Niknia et al., (2020); Chen and Zhang, (2019)]

2.6 Carbon dots (CDs) loaded Functional Aerogel

Active nanomaterials like quantum dots (QDs), carbon dots (CDs), and others are being used to make functional aerogel. Mostly CDs are used for sensing and detecting a specific material (like, pesticide residue in food stuffs, volatile organic compounds, etc.). CDs based sensing and detection techniques are fully based on their fluorescence behaviour. Moreover, one of the most beseeching detection techniques is solid-state fluorescence sensing as it is very simple and convenient in terms of practical application. However, CDs based solid-state fluorescence sensing is limited by their dried powder form as CDs form aggregates, which ultimately induce quenching of fluorescence of CDs. Commonly, grafting of CDs in a solid matrix (silica, urea polymer etc.) is an effective way to overcome the undesirable problem (Ma et al., 2019). Therefore, aerogel are reported to be as emerging material in the said prospect (**Table 2.7**).

2.6.1 Synthesis of CDs

CDs are quasi-zero dimensional material of nearly spherical shape with particle size less than 10 nm. CDs seems to have an amorphous or crystalline core with sp^2 hybridized carbon atom predominantly and the surface contains carboxyl groups (Liu et al., 2017). However, mostly CDs are amorphous which consists of sp^2 and sp^3 hybridized carbon atoms with two other fundamental elements namely hydrogen and oxygen (Bhartiya et al., 2016). CDs have been developed by Xu et al. (2004) accidentally while synthesizing single-walled carbon nanotubes through applying arc discharge. Currently, researchers are putting tremendous effort in the development of CDs to replace toxic metal originated (QDs) as it causes potential health and environmental hazard (Khairol Anuar et al., 2021). Generally, CDs are synthesized by following two routes (i) top-down and (ii) bottom-up method. The top-down method develop CDs by peeling or breaking carbon rich structures (Wang and Hu, 2014). The techniques followed in top-down method are arc discharge, laser ablation, chemical oxidation, electrochemical oxidation etc. In bottom-up method, CDs are synthesised from small carbon rich molecules like, citric acid, ethylene glycol, glycerol, citric acid with amino compounds etc. (Sharma and Das, 2019). The techniques involved in bottom-up method are hydrothermal synthesis, microwave heating, pyrolysis, combustion, etc. Bottom-up method of CDs development are very popular as these are simple, economic, environment friendly, etc. (Vervald et al., 2025). However, separation and purification of CDs from synthesized complex mixture is important. Centrifugation, solvent extraction, dialysis etc. techniques are generally employed to obtain CDs in pure form (Mohammed et al., 2023).

2.6.2 *Loading of CDs in aerogel*

Based on the literature, loading of CDs into the aerogel matrix can be done through adding CDs either at the early stage of aerogel making (Zhang et al., 2020) or at the end of aerogel making (Wu et al., 2019) (**Fig. 2.4**). More specifically, physical and chemical bonding anchors the CDs grafting and decides the loading efficiency including leaching of CDs (Quraishi, Plappert, Grießer, & Liebner, 2019). It is noteworthy to mention that the grafting technique is the ultimate factor which decides the loading capacity of CDs, more specifically, how CDs are interacting (physical, chemical interaction, etc.) with the aerogel material. For example, carboxyamine condensation between carboxyl group of CNF and amino group of surface modified CDs develops strong covalent bond which gives structural stability to the CDs loaded aerogel in comparison to pure CNF aerogel. Moreover, optimum CDs grafting facilitates to achieve higher compressive strength and maintaining porous microstructure through avoiding disintegration in water (Wu et al., 2019). Wu et al. (2019) reported the highest CDs grafting content (113 mg CD/g of CNF aerogel) for the aerogel CNF/CD-3% on the basis of UV absorption and gravimetric measurement. Zhang et al. (2020) observed the formation of hydrogen bonds between Ln^{3+}-T complex and CDs which present loose, porous and interconnected structure of Ln^{3+}-T/CDs aerogel. They achieved highest quantum yield of 47.4 % through eliminating hydration between lanthanide ions and water molecules. Quraishi et al. (Quraishi, Plappert, Grießer, & Liebner, 2019) observed higher loading capacity of CDs in final hybrid aerogel matrix due to aqueous carbodiimide coupling of surface amino modified CDs. Physical (electrostatic interaction) and chemical bonding (covalent coupling) approach confirms excellence of covalent grafting. Therefore, these observations suggest that selection of effective and efficient grafting technique results in good loading capacity of CDs with negligible leaching subjected to different condition (compression, tension, etc.). The grafting approaches (**Table 2.7**) are explained in the following paragraphs.

2.6.2.1 *Loading of CDs prior to aerogel formation*

Based on the studies (i.e., addition of carbon dots before aerogel making), either previously synthesised CDs are added with the aerogel precursor material (direct addition) or CDs precursor is added with the aerogel precursor (indirect addition) and eventually the end product is obtained through following further processing operations.

2.6.2.1.1 *Direct addition of CDs*

The loading of CDs at different stages of aerogel development is depicted in **Fig. 2.4**. Quraishi et al. (Quraishi, Plappert, Grießer, & Liebner, 2019) reported grafting of surface

passivated (amino groups) CDs after synthesising it separately through co-hydrothermolysis (microwave assisted) of orange juice and 2,2-(ethylenedioxy)-bis-(ethylamine) (EDEA). Firstly, the authors have followed acid-induced gelation of aqueous dispersion of carboxylated individualized cellulose nanofibers (*i*-CNF) to obtain hydro-alcogels which were then submerged in HCl (1mM) for 24 h. Finally, loading of CDs has done through transferring the gels into a loading bath containing CDs with identical HCl (1mM) solution. Eventually, the CDs loaded hydrogel is converted to aerogel through super critical CO_2 followed by consecutive solvent exchange steps. The loading of CDs is done through ionic bonding in which physical immobilization of CDs takes place under controlled pH and electrostatic attraction between ammonium and carboxylate ions. Moreover, electrostatic repulsion is reduced between *i*-CNF due to protonation of carboxyl groups executed by hydrogen bonding and inter-nanofiber van der waals forces. Secondly, the authors have also reported covalent grafting of surface modified CDs through traditional N-(3-dimethylaminopropyl)-N′-ethylcarbodiimide hydrochloride (EDC)/N-hydroxysuccinimide (NHS) carbodiimide coupling chemistry. In both grafting mechanism, part of the loaded CDs works as anchor sites to establish inter-particulate cross-links to carboxyl groups present on the surface of *i*-CNF. While comparing both of these techniques of grafting, it will be noteworthy mentioning that chemical grafting produces undesirable by-products (nonhomogeneous gel clusters of cross-linked multiple numbers of *i*-CNF through surface modified CDs) which is difficult to remove from gel state however, prior to gel formation this grafting technique can be accepted as an alternative approach. Moreover, due to process simplicity and less volumetric shrinkage during alcogel formation physical grafting is widely accepted (Gogoi et al., 2015). Zhang et al. (2020) have reported the addition of separately developed CDs in to aerogel precursor solution (lanthanide (Eu^{3+} and Tb^{3+}), thymidine and de-ionized water). The hydrogel (Ln^{3+}−T/CDs) has been formed through simple coordination and self-assembly process. Finally, freeze drying technique is used to convert hydrogel into aerogel. CDs, which contains hydroxyl and carboxyl groups, are grafted inside the aerogel matrix through formation of intermolecular hydrogen bond between Ln^{3+}−T and CDs. Sun et al. (2021) reported fabrication of cellulose based carbon aerogel. CDs were produced separately from the mixture of folic acid, adenosine triphosphate (ATP) and *N*,*N*-dimethylformamide (DMF) using an autoclave. Mixture of cellulose, graphene oxide (GO) and CDs were ultrasonicated to develop a homogeneous suspension, then it was frozen by bidirectional freeze casting prior to freeze drying. Bidirectional freeze casting leads to incorporation of reduced (r) GO-CD-carbon microfiber (CMF) sheets of uniformly decorated

CDs into the aerogel matrix and rejects the formation of unique bridged lamellar structure due to formation of ice crystals. Moreover, a continuous and regular parallel lamella of rGO-CD-CMF with micrometer size range was developed. CDs promotes uniform distribution of N and P into the aerogel matrix. Finally, the aerogel was formed and later it was carbonized using furnace with N_2 flow to form carbon aerogel. Yuan et al. (2020) developed CDs (synthesized from citric acid) based carboxy-methylated cellulose nanofibrils (CM-CNF) fluorescent aerogel. CM-CNF was also prepared using eucalyptus kraft pulp and further it was modified with the previously developed CDs. CDs were grafted onto CM-CNF using simple chemical grafting technique (EDC/NHS coupling chemistry; Quraishi et al., 2019). Chemical crosslinking between CNF and CDs leads to form CM-CNF-CDs. Hydrogels were obtained through free radical polymerization and were further converted into aerogel through freeze drying. Ma et al. (2019) developed CDs based aerogel for the detection of aniline gas. CDs were prepared separately from sawdust using hydrothermal process (one-pot carbonization) and were mixed with tetraethyl orthosilicate (TEOS) to form CDs-silica aerogel composite through one-step sol-gel method. The surface of the obtained CDs is rich in hydroxyl groups which promotes gelation process of TEOS and reduced the gel time. The author hardly finds CDs from the TEM (Transmission Electron Microscopy) images, as they were coated during silica gel process, more specifically, maybe due to formation of intermediate product against reaction with TEOS.

2.6.2.1.2 *Indirect addition of CDs*

Precursor of CDs are added with the precursor of aerogel at the initial stages of aerogel formation rather adding the synthesised CDs directly (**Fig. 2.4**). The synthesis of CDs and formation of aerogel is carried out simultaneously. The indirect addition of CDs was followed by Wang et al. (2020) to develop phosphorous (P) doped carbon dot/graphene aerogel using single step hydrothermal process. In aqueous dispersion of graphene oxide (GO), phytic acid is dispersed to serve as a source of P as well as precursor of CDs. The chemistry behind the formation of this nanocomposite through a single step hydrothermal synthesis is conversion of phosphorous acid arms into organophosphates due to carbonization of phytic acid, further phosphate linkage formation generates polymeric layer. More specifically, one way it forms the molecular network of CDs geometry through phosphate linkages between polymeric layers and in another way intermediate phosphate linkages anchors with the non-homogenous low energy sites to form stable state. Moreover, GO surface contains highly active sites due to presence of graphene defects or oxygen atoms, which is substituted by phosphate linkages or

combined directly with defective carbon atoms to form P-C bonds that enables settling of phytic acids molecular framework on the surface of GO, afterwards it was converted to CDs. Eventually, final product is obtained through high temperature annealing process.

2.6.2.2 *Loading of CDs into developed aerogel*

In this approach, CDs precursors or previously synthesized CDs were loaded directly into the aerogel matrix which were developed separately (**Fig. 2.4**). Dolai, Bhunia, and Jelinek (2017) reported development of CDs based aerogel for sensing of volatile compounds. Silica aerogels are separately formed in a furnace in N_2 gas atmosphere using TEOS as precursor material of aerogel. High temperature annealing of silica aided with pressurized N_2 gas leads to form porous aerogel matrix. Synthesized CDs from 6-*O*-(*O*-*O*′-dilauroyl-tartaryl)-D-glucose was added into the previously developed aerogel, then the suspension was sonicated, heated, and purified. The CDs precursor material was expected to be efficiently adsorbed and immobilize into the pores of aerogel matrix due to amphiphilic surface domains of aerogel pores and amphiphilicity of the CDs precursor material. Wu et al. (2019) developed CDs and nanocellulose based fluorescent aerogel for optical sensing. Cellulose nanofiber-based aerogel was developed separately through freeze drying process; however, amino modified CDs were developed by hydrothermal treatment using organic citric acid and branched polyethyleneimine (PEI) mixture. Finally, to obtain CDs and CNF based aerogel, pure CNF aerogel was dipped into aqueous suspension of amino modified CDs. Chemical grafting technique was used herein to load the CDs. Condensation reaction between amino group of CDs and carboxyl group of CNF forms covalent bonding which provides structural stability to the aerogel. The reaction was initiated by the addition of EDC and NHS and complete reaction (external to internal aerogels) was obtained in incubator shaker through rigorous shaking.

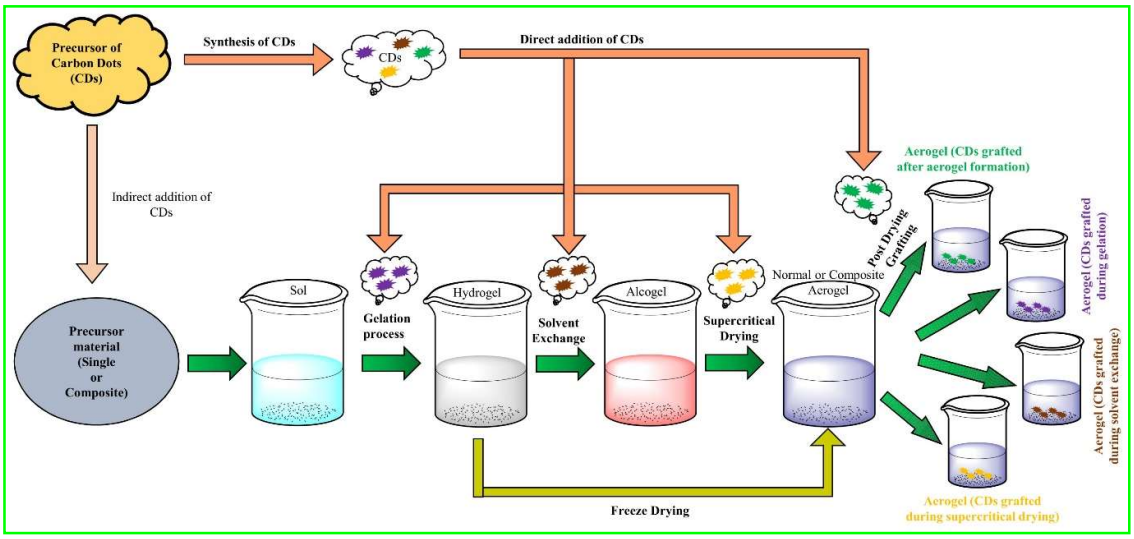

Fig. 2.4 Loading of carbon dots (CDs) at different stages of aerogel preparation

2.6.3 *Characterization of CDs based aerogel*

2.6.3.1 *Morphological characterization*

The particle size of CDs used in prepared aerogels are generally confirmed by TEM, particle size analyzer, atomic force microscopy (AFM) and dynamic light scattering instruments. AFM is the technique in which forces between probe and sample reveal the topography with high resolution. AFM of the CDs synthesized by microwave treatment from lemon extract revealed that CDs had an average size of 1.8 ± 0.75 nm (Quraishi, Plappert, Grießer, & Liebner, 2019). The topography, more specifically the internal porous network of aerogel is determined and confirmed by performing SEM (scanning electron microscopy) analysis. The surface characterization such as specific surface areas and pore structures of the aerogels are found using gas adsorption and desorption in BET (Brunauer-Emmett-Teller) instrument (Yun et al., 2019). The XRD (X-ray diffraction) analysis reveals the crystallinity/amorphous nature of the CDs used in aerogels. HRTEM (High-resolution transmission electron microscopy) is high resolution TEM in which contrast of phase is utilized from transmitted and scattered electrons to provide images with high resolution. HRTEM analysis of CDs doped gel reveal the particle size of CDs from wood powder as 6-8 nm (Song et al., 2020). SEM analysis of CDs-aerogel made for VOC (Volatile Organic Compound) detection show that there is more surface area organization (Lee et al., 2002). The CDs shows broad peak at 25.1° for (200) plane of disordered graphitic like structure and CDs-graphene aerogel shows broad peaks around 24.5° corresponding to (002) plane when analyzed by XRD (Wang et al., 2018). The BET analysis shows that specific surface area of CNF aerogel increased to >100 m^2 g^{-1} with the addition of CDs (3, 3.5, and 4 %) while preserving light weight and retaining the porosity and apparent

density of aerogels of about 98.5 % and 0.02 g/cm^3 respectively (Wu et al., 2019). The morphological advantage of the CDs, owing to their small size, are harnessed in nano-level applications of bio imaging, delivery, and sensing.

2.6.3.2 *Functional characterization*

It's necessary to know the functional and chemical composition of aerogels after formation of the structure to confirm the presence of bonds between composites and CDs in aerogels. For the sawdust CDs-silica aerogel, the antisymmetric stretching vibration and symmetric stretching vibration of Si-O-Si are found at the peaks of 1078 cm^{-1} and 798 cm^{-1} respectively. The peaks at 3446 cm^{-1} and 1661 cm^{-1} represent O-H antisymmetric stretching vibration and O-H bending vibration respectively, and the peak around 954 cm^{-1} corresponds to the stretching vibration of Si-OH (Ma et al., 2019). EDS (Energy disperse X-ray spectroscopy) is a micro-analysis technique in which X-rays cause excitation in the sample due to which energy difference occurs and X rays are emitted from which elemental composition is determined. The EDS spectrum in CQD (carbon quantum dot)/reduced Graphene Oxide/Fe_2O_3 composite aerogel shows the presence of Fe, O, C, and N elements in them and EDS elemental mapping proves as evident for the formation of composite structure in aerogel (Yun et al., 2019). In CQD-nanofibrillated cellulose aerogel, C–C, C–N, C–O, and C=N/C=O bonds are confirmed by the peaks at 284.6eV, 285.7eV, 286.6eV, and 288eV and N1s peak at around 396eV confirms the composite-CQD formation. For C–N–C, N–H, -NO_3 bonds, peaks are found at 399.1 eV, 401.1 eV and 406.2eV respectively (Song et al., 2020). In the thenoyltrifluoroacetone (TTA)-CDs aerogel, Raman signal is more intense at 1526 cm^{-1} due to intensity changes and fluorescence shifts caused by the interaction with UO_2^{2+} or Sm^{3+} ions (Dolai, Bhunia, Zeiri, et al., 2017). In ^{1}H NMR spectra of light emitting aerogel doped with lanthanide/thymidine/CD, peak is broadened because of the paramagnetic effect of Eu^{3+} and Tb^{3+}. The bond between Ln^{3+} and thymidine was evident from the disappearance of furanose ring at 4.6 ppm, Ln^{3+}-T complex exhibits a broadened peak (in between 3100-3500 cm^{-1}) due to formation of intermolecular hydrogen bonding (Zhang et al., 2020).

2.6.3.3 *Optical behavior*

CDs based aerogel possess excellent photo luminescent (PL) properties finding its applications in optical sensing. Hence, it's important to characterize the optical behavior of these aerogels. The quantum confinement effect where energy gap is based on CDs size and shape is accepted as the main mechanism for PL of CDs (Zhao et al., 2020). Optical characterization is done by UV-visible spectroscopy and fluorescence spectroscopy. For CDs-

Graphene aerogel, CDs had a broad peak in the UV region and a tail in the near-visible region, displaying various π-π* (C=C) and n-π* (C=O) transitions (Wang et al., 2018). The Photoluminescence spectroscopy showed typical excitation-wavelength dependent behavior for the excitation wavelengths of 320 to 480 nm. Based on this, it was proposed that CDs containing aerogel could act as UV–vis light photosensitizer. For the CDs/PVA aerogel, He et al. (2018) found that π-π* transition from the C=C bonds and n-π* transition from the C=O bonds are present at 253 nm and a broad range at 350 nm, respectively in the UV-vis spectrum. When examined using PL spectroscopy, it's found that the CDs showed only fluorescence and quite weak phosphorescence. PL spectra of CD/PVA reveals that it has emission peak at 450 nm showed blue color emission (He et al., 2018). Ln^{3+}-T/CDs aerogel exhibit broad range of luminescence (purple to red) while tailoring the stoichiometric ratios of Eu^{3+}, Tb^{3+}, and CDs. At an optimum stoichiometric ratio of Eu^{3+}, Tb^{3+}, and CDs (1:199:33), the aerogel emits white light (Zhang et al., 2020).

2.6.3.4 *Responsiveness to different stimuli*

CDs aerogels are sensitive to different stimuli such as temperature, pH, and humidity, thereby could be of potential use as sensors.

2.6.3.4.1 *pH responses*

At different pH the CDs based aerogel shows different responses to PL intensity. PL intensity changes drastically at both the extreme pH (lowest (2) and highest pH (12)) conditions however, in the intermediate pH (4, 6, 8, and 10) negligible changes in PL intensity was reported (Wang et al., 2022). At lowest pH the PL intensity was highest whereas, it reflects lowest intensity value at highest pH value. The reduction of PL intensity may be attributed to fluorescence quenching due to accumulation of negative charge density on the surface which affect the π-π* and n-π* electron transfer. However, at lowest pH the acidic property was endowed by the presence of oxygen-containing groups on the surface in ample amount (Wang et al., 2022). Zhang et al. (2020) reported that for white light emitting CDs based aerogel at acidic pH, PL intensity decreased due to dissociation of Ln^{3+}T complex with the addition of H^+, showing blue fluorescence. When OH^- was added further, PL recovery didn't occur. At neutral pH, luminescence was recovered. Photoluminescence (PL) response of CDs used in aerogel was largely insensitive towards pH changes from 6 to 12 but a significant reduction of PL intensity was observed below pH 3 (Quraishi, Plappert, Grießer, & Liebner, 2019). Song et al. (2020) studied the adsorption performance of aerogel at various pH. They reported that the 6 is the optimum pH at which adsorption performance is strongest and it decreased along with

PL intensity under low pH since carboxyl, aldehyde, and amino groups present on surface adsorption sites combine with H^+ ions. The aforesaid observation was supported by Jing et al. (2022) during adsorption performance of Cr^{6+} using CDs based aerogel.

2.6.3.4.2 *Temperature responses*

Temperature is an important parameter which can alter the rate of removal of target metal ions and adsorption capacity of the CDs aerogel. The increase in temperature increases the removal rate and adsorption capacity. The temperature increase is conducive to reaction (Jing et al., 2022). Zhang et al. (2020) reported that the prepared CDs-aerogel showed high PL at 417 nm when increased from −20 to 80°C and then gradually reduced due to defects or ionic impurities. Moreover, Jing et al. (2022) performed experiment at 52°C through optimization for subsequent adsorption. The aerogel also showed reversible responsiveness.

2.6.3.4.3 *Humidity responses*

Zhang et al. (2020) reported that the luminescence of the prepared aerogel changed from white to violet-blue gradually. When subjecting the aerogel for 20 min to steam, the PL intensity of CDs increased by 57% due to their water solubility. It is proposed that this aerogel could be used as a humidity-sensing material, finding application in determining the human breath's humidity change. Dolai, Bhunia, Beglaryan, et al. (2017) experimented with the prepared CDs aerogel for humidity responses. It was found that there were insignificant fluorescent intensity changes in a broad range of humidity. Only gas induced fluorescence quenching was observed at various humidity ranges.

2.6.3.4.4 *Impact of interaction with different compounds/ions*

The PL intensity of the WLE (White Light Emitting) aerogel varies upon interaction with different halide ions at different concentration. Halide ions like $Cl^–$, $Br^–$, $I^–$ showed no significant change in PL whereas it was increased by F^- at emission peak of 417 nm due to hydrogen bond (Zhang et al., 2020). On interaction with cations such as Na^+, K^+, Mg^{2+}, Ca^{2+}, Mn^{2+}, Zn^{2+}, Ni^{2+}, Fe^{3+}, and Al^{3+}, insignificant PL intensity change occurred. Dolai, Bhunia, Zeiri, et al. (2017) studied the interaction of TTA/CDs aerogel with metal ions. Among the metal ions, only UO_2^{2+} showed high fluorescence shift with LOD <10 ppm. It was found that ion concentrations and fluorescence quenching are directly proportional due to adsorption of the ions inside the pores of the aerogel pores. The bond between ions and TTA units at the CDs surface causes changes in their surface energy states due to which quenching occurs (Dolai, Bhunia, Zeiri, et al., 2017).

Yun et al. (2019) developed a Fe_2O_3 modified N doped CDs/Graphene aerogel as anode material for batteries. N doping CDs in aerogel causes nitrogen atoms to give lone electron pairs to the π-conjugated CDs (Wang, Wang, et al., 2018). So it creates more defects in the CDs/rGO composite aerogel, thus more electroactive sites are available thereby increasing specific capacity and electronic conductivity of the composite aerogel (Yun et al., 2019).

2.6.3.5 *Mechanical properties*

Sun et al. (2021) constructed lamellar cellulose-based carbon aerogels with CDs for water deionization and energy storages. Carbon aerogel, due to its high compression properties and high electrical conductivity is an excellent elastomer. It is compressible and of light weight due to interconnected bridges which act as springs and hold every parallel layer. The R/R_0 (compressive stress / compressive strain) of the carbon aerogel shows high stability in the 20 cycles of the cyclic compression test at 50% strain thus possess longer duration stability.

Quraishi et al. (2019) studied the grafting techniques for CDs/hybrid aerogel. They found that Young's modulus of the materials obtained by chemical bonding of CDs was almost more than twice as high as for the reference aerogels. This is owed due to the higher density of the hybrid aerogels and covalent bonding. The yield point is also almost twice as high compared to aerogel physical bonding method. The chemical grafted aerogels are more elastic than that of the physical bonding and also have higher resilience. Sun et al. (Sun et al., 2021) reported CDs loaded carbon aerogels have better mechanical stability as compare to the cellulose based carbon aerogels. The aerogel can resist collapse even after 20 consecutive compressions with 50 % strain. The reason behind the deformation without collapse and more compressible nature of the aerogel is attributed as the spring like action of interconnected bridges. CDs based aerogel with such mechanical properties (reliability and working life) opens new field of application.

2.6.4 *Application of CDs loaded aerogel*

CDs based aerogels got diverse range of applications (**Table 2.7**) in various fields due to their unique characteristics and environment friendly nature. Various applications of CDs based aerogels are given below.

2.6.4.1 *Photosensitizer*

Photosensitization is the process in which a physicochemical change occurs by donating an electron to the substrate or by abstracting a hydrogen atom from the substrate and UV light is absorbed in the process. Wang et al. (2018) developed a 3D CDs/graphene aerogel (GA) with

improved photosensitization property due to the multidimensional electron transport pathways.The 3D GA structure not only acts as support for immobilizing CDs but also helps to transfer carriers of charge from CDs, thus enhancing photosensitization. Moreover, 3D GA makes it feasible to recycle the water-soluble CQDs from liquid-phase reaction system. The optimal photocatalytic activity of the CQDs/GA aerogel is found to be 2.59 times higher than that of only CQD. It is of potential to be used as renewable photocatalysts for solar energy conversion. He et al. (2018) constructed a Graphene-CQD/g-C_3N_4 nanosheet aerogel for photocatalytic removal of organic pollutant with inexhaustible solar energy. CQDs and reduced graphene oxide improved the visible light absorption and paved way for the separation of charges. The ternary structure of reduced graphene oxide enhanced support for 3D network, enhanced photocatalytic activity and stability of aerogel for longer duration. Another important application of photosensitization characteristics of CDs based aerogel is solar water evaporation. The CDs plays major role in water activation which is the basis of water evaporation. The reduced water evaporation enthalpy accelerates the water evaporation process. It may be attributed to the presence of oxygenated groups in the aerogel. The structural and compositional properties of the CDs based aerogel regulates the water evaporation performance as these properties are directly related to (i) superiority in reducing water evaporation enthalpy, (ii) enhanced light harvesting, and (iii) effective energy and water management (Xu et al., 2022). Xu et al. (2022) reported high water evaporation rate (2.29 kg $m^{-2}h^{-1}$) with a good energy conversion efficiency of 93.5 % during their study. Moreover, the CDs based aerogel developed by Xu et al. (2022) showed stable water evaporation rate in alkaline, high-salt (10 wt %), acidic, and organic pollutant solution also.

2.6.4.2 *Air pollutants sensing*

Nitrogen dioxide is a common air pollutant from traffic. It is capable of creating many negative health and environmental impacts (Boningari & Smirniotis, 2016). Exposure to NO_2 for a long time poses higher risk for death due to cardiovascular and respiratory issues (Huang et al., 2021). Prinz and Richter (2022) found through their research work that there is possible correlation between long-term fine particulate air pollution and increasing spread of COVID-19 cases. Functionalized silica aerogels with the branched polyethylenimine capped carbon dots as gas sensor for the detection of NO_2 were reported (Wang et al., 2013). High immobilization and stability was achieved between branched polyethylenimine-capped carbon dots (BPEI-CDs) and supercritical fluid extracted silica aerogel by strong electrostatic interaction between the positively charged PEI polyelectrolytes present on the surfaces of the

CDs and the negatively charged silica surfaces of silica aerogel (Borkovec & Papastavrou, 2008). The NO_2gas is detected with high selectivity by strong fluorescence quenching of the aerogel by NO_2 with limit of detection of 250 ppb concentration (Wang et al., 2013). The fluorescence quenching could be attributed to the interaction between electron-donor polyethylenimine and electron-acceptor NO_2 (Kuzmych et al., 2007).

Volatile organic compounds (VOC) are atmospheric pollutants that cause negative effects on human health (Montero-Montoya et al., 2018; Zhang et al., 2022). Dolai, Bhunia, and Jelinek (2017) developed an inexpensive vapour sensor for detecting aromatic VOCs using silica aerogel embedded with fluorescent CDs. Here, the carbon precursor 6-O-(O-O′-dilauroyl-tartaryl)-D-glucose was encapsulated within the aerogel matrix, and heating of the composite material generated the CDs aerogel vapor sensor. Aniline and p-phenylenediamine showed fluorescence quenching, and with vapors of the other aromatic VOCs it was low or negligible quenching (Dolai, Bhunia, & Jelinek, 2017).

Wu et al. (2019) developed an optical sensor using nanocellulose- CDs aerogel for water/air quality monitoring by detecting nitric oxide gases and aldehydes. The nitric oxide gases are detected by the strong fluorescence quenching of the developed aerogel by the adsorption of these gas molecules in the pores of aerogel thus preventing the radiative recombination of electrons from the interaction between electron-donating CDs and electron withdrawing NOx molecules (Dong et al., 2013). Aldehydes are detected by fluorescence quenching occurring through the covalent reactions between aldehyde groups and surface amino groups of CDs that causes the lowering of fluorescence excitation through the adsorption of aldehyde groups (Wu et al., 2019). Ma et al. (2019) developed a CDs-silica aerogel solid fluorescent material for selective detection of aniline gas by fluorescence quenching of efficiency up to 76.4%.

2.6.4.3 *Heavy metals detection*

The rapid development of agriculture and industry leads to increase in the amount of chemical residue with the use of enhanced number of chemical products. Now a days growing utilization of Lanthanides and actinides (Ln and An) in nuclear reactors, medical fields and industries pose threat to human health and environment. Another toxic heavy metal ions like Cr^{3+}, Cr^{6+}, etc. are very harmful to aquatic organisms as well as human beings directly through drinking water, skin contact or through food pathways (Song et al., 2020; Jing et al., 2022). CDs based aerogel as a carrier of CDs played an important role in sensing as well as adsorption of metal ions as the aerogels having porous structure with high surface area which accepts rapid

and easy adsorption of metal ions. Dolai, Bhunia, Zeiri, et al. (2017) constructed a fluorescent sensor using 2-thenoyltrifluoroacetone (TTA) CDs-silica aerogel hybrid for detection of UO_2^{2+}, Sm^{3+}, and Eu^{3+}. TTA is a very selective ligand for cross-linking with An and Ln ions. This TTA CDs based aerogel enabled the detection of UO_2^{2+} ions by red fluorescence shift, Eu^{3+} and Sm^{3+} ions by fluorescence quenching (Dolai, Bhunia, Zeiri, et al., 2017). Adsorption performance of CDs based aerogel is influenced by the pH and ion concentration of the medium. In acidic condition adsorption is very less due to increase in degree of protonation of functional groups on the surface of CDs and the H^+ ion occupies the active sites of composite. Maximum adsorption of metal ions was reported on pH 6.0 (Song et al., 2020; Jing et al., 2022), beyond that pH adsorption capacity decreases. The adsorption capacity increases with the increase in ion concentration of the solution.

The adsorption experiment of Cr^{3+} and Cr^{6+} was performed by Song et al. (Song et al., 2020)& Jing et al. (2022). Song et al. (Song et al., 2020) constructed a CQD- nanofibrillated cellulose (NFC) composite aerogel by green synthesis which detects Cr^{3+} ions in water. NFC aerogel has very high adsorption capability (Wan et al., 2015), the amount of NFC aerogel adsorption of Cr^{3+} had positive correlation with the fluorescence quenching of CQD and fitted pseudo second order kinetics well (Song et al., 2020). Carboxy-methylated cellulose nanofibrils (CM-CNFs) and CDs were used by Yuan et al. (2020) during synthesis of CDs based fluorescent aerogel to adsorb Cr(VI) metal ion.

2.6.4.4 *Energy storage*

Carbon aerogel of reduced graphene oxide (rGO) and carbon microfiber (CMF) with CDs was synthesized for excellent energy storage and capability of deionizing water (Sun et al., 2021). Carbon materials have high conductivity, porous structure, chemical stability (Liu et al., 2020). Therefore, they could be a good source for aerogel of storage applications. Carbon quantum dots were doped with N, P, O which act as electron-rich regions, aiding for electron transport without compromising stability and specific surface area. The CDs act as a bridge to connect the other composites (Lv et al., 2018). The aerogel has very good compressibility (up to 80 % strain) due to unique bridged layered structure of the composite developed through bidirectional freeze-casting. This carbon aerogel will be able to light an LED in series connection. With the incorporation of CDs, 117% increase in specific capacitance and 31% improvement in deionization capacity is found when compared with the aerogel without CDs, thus highlighting that CDs could be used in electrodes for storage and deionizing purposes.

Nitrogen-doped CQD/reduced graphene oxide/porous Fe_2O_3 (N-CQD/rGO/Fe_2O_3) composite 3D network aerogels which are green, renewable energy sources were developed (Yun et al., 2019). The high porosity of the structure increases the charge storage, thus improving the specific capacity of Fe_2O_3 (Zhang et al., 2013). The electrical conductivity of the developed aerogel is increased by the CQD and N doping. CQD is a good conductive agent and prevents the agglomeration of rGO by acting as intercalator which causes the increase in specific capacity. N doping increases the electroactive sites thus increasing the specific capacity and electronic conductivity.

2.6.4.5 *Potential food applications of CDs based aerogel*

Based on fluorescence quenching of CDs based aerogel most of the detection method was established. The specific detection of the target material paves the way of application of CDs based aerogel in food and agriculture. The detection of Fe^{3+} and Vitamin C in fruits through an "on-off-on" sensor made of chitosan and glycine hydrochloride ionic liquid (IL) is of great importance. This carbon aerogel based "on-off-on" sensor works on the basis of diminishing and restoring of fluorescence. The presence of electron rich groups (-NH_2, -OH) on the surface interacts with Fe^{3+} with higher binding affinity and forms aggregate by chelating with -NH_2, -OH groups hence, fluorescence quenched. Interestingly, after addition of Vitamin C the quenched fluorescence is partially recovered. This may be attributed to redox reaction (between Fe^{3+} and Vitamin C) which reduces Fe^{3+} to Fe^{2+} (having less chelating ability unlike Fe^{3+}) and converts hydroxyl group of Vitamin C into ketone (Wang et al., 2022).

Ehtesabi et al. (2019) developed CDs encapsulated in sodium alginate hydrogel for tetracycline (TC) sensing in food samples and environment. TC is detected by fluorescence quenching of CDs in hydrogel using smartphone-based fluorimeter. Fluorescence quenching of CDs takes place due to formation of complex upon interaction between TC and functional groups (carboxyl and hydroxyl) present on the surface of CDs. Theelectronic structure of CDs may have changed due to formation of complex which facilitates the nonradiative recombination of the excitons through an effective electron transfer process (Ehtesabi et al., 2019). The hydrogel can be used both as adsorbent for environmental TC pollutants and as TC detector. Its potential use as an aerogel sensor, as aerogel could be obtained from hydrogel by processes like supercritical fluid extraction, freeze drying (Ciftci et al., 2017).

Another important application of CDs based aerogel is organophosphate pesticides (OP) detection in agricultural products. The detection method is also based on fluorescence

quenching. Hu et al. (2019) constructed a fluorescence microfluidic CdTe aerogel along with acetylcholinesterase enzyme (AChE) for sensing OP. The sensor detects by measuring fluorescence intensity quenching change of QDs aerogel due to the hydrolytic reaction of acetylthiocholine (ATCh) catalyzed by the AChE, and again fluorescence is recovered based on lowered enzymatic activity. The hydrolytic reaction of ATCh forms acetate and thiocoline. The photoexcitation of CdTe QDs generate holes in the valence band, thiocoline acts as donor and thus PL quenching of QDs aerogel takes place. However, when OP is added, it interacts with the active centre of AChE and the enzyme activity is decreased thus thiocholine production is inhibited and fluorescence is recovered. Therefore, the concentration of OP can be detected on the basis of PL intensity of QDs aerogel. The sensor's LOD (Limit of detection) is reported as 0.38 pM. The sensor showed similar quenching for various pesticides due to its 3D porous aerogel nano-structure. So, it's a potential sensor as CDs-aerogel where CdTe could be replaced by CDs in this developed aerogel. This is a rapid, accurate, and cost-effective detection method having high sensitivity with large detection range.

Ascorbic acid (AA) is a very important vitamin, inadequate consumption of this vitamin leads to scurvy. AA as an antioxidant is widely used in food, animal feed, beverages and pharmaceutical formulations. The selective sensing of AA is necessary as its application is growing in the field of food and medical. On the other hand, hydrogen peroxide (H_2O_2) is used as an analyte in some fields like, chemical, pharmaceutical research, alimentary industries and clinical laboratory however, it is very dangerous to human health as it causes serious health issues like aging cancer, cells and neurodegenerative processes. To detect AA and H_2O_2, Wang, Hei, et al. (2019) developed a low-cost carbon nanorods assembled hierarchical meso-macroporous carbons networks aerogels (CNs-HMCNAs) apples for detecting ascorbic acid and hydrogen peroxide. This aerogel possessed meso-macroporous structure with high specific surface area and lot of edge defective sites, thus electron transfer between the glassy carbon electrode (GCE) and the ascorbic acid (AA) (or hydrogen peroxide (H_2O_2)) was efficient. The interference effect investigated by amperometry to know the selectivity of the material for AA detection. The apparent increase in electrooxidation current indicates the selectivity to AA. However, apparent increase in electroreduction current and anti-interference property are the fundamental parameters in selective detection of H_2O_2.This aerogel could potentially be incorporated with CDs for detection. This aerogel could be potentially used in the practical determination of acetic acid in fruit juices or H_2O_2 detection in milk and beer.

Many CDs have been shown to exhibit antimicrobial and antioxidant activities, which can be used in packaging materials to inhibit microbial growth and chemical deterioration of foods (Moradi et al., 2021). Bio-composite films from cassava starch incorporated with cinnamaldehyde through super-critical solvent impregnation which could be utilized as active packaging for food since cinnamaldehyde possess antimicrobial activity (Cristina et al., 2014). This film could potentially be developed as CDs based aerogel by modifications to be as active packaging. Koshy et al. (2021) reported the development of pH sensitive intelligent starch based biopolymer film by incorporating CDs and anthocyanin extracted from *Clitoria ternatea* flower for monitoring freshness of spoilage of pork based on checking levels of total volatile basic nitrogen which would be generated in spoiled pork. Similar approach could be done for CDs based aerogel for packaging. CDs based aerogel could potentially be used in active packaging due to their UV barrier properties as reported in previous studies (Hess et al., 2017; Yang et al., 2019).

Table 2.7 Carbon dots (CDs) based aerogel, their characteristics and application

CDs precursor material	Method of CDs synthesis	Size of CDs (nm)	Grafting mechanism	Stage of grafting	Precursor material	Drying method	End properties of aerogel		Application
							SSA (m^2/g), ε (%), ρ (g/cm^3)	Quantum yield (%)	
Phytic acid	Hydrothermal treatment	NR[#]	Chemical (through phosphate linkages)	Before aerogel formation	Graphene	Hydrothermal, Annealing	448.24, NR[#], NR[#]	NR[#]	Liquid Al–air battery, all-solid-state flexible Al–air battery
Lemon juice	Microwave-assisted cohydrothermolysis	1.8 ± 0.75	Ionic and Chemical bonding (EDC/NHS carbodiimide coupling chemistry)	Before aerogel formation	Cellulose nanofibers	$SCCO_2$	345-491, -, 0.0163-0.0201	NR[#]	Environment friendly chemical sensing and volumetric display
ATP and folic acid	Solvothermal method	3.87	Chemical (pyridinic and pyrrole attachment)	Before aerogel formation	Microfibrillated cellulose, GO	Freeze drying	559-601, NR[#], NR[#]	NR[#]	Superior energy storage and water deionization
Citric acid	Hydrother	NR[#]	Chemical	Before	CM-CNF	Freeze	NR[#], NR[#], NR[#]	11.8	Adsorbent and

	mal method		bonding (EDC/NHS carbodiimide coupling chemistry)	aerogel formation		drying			sensitive optical sensor of Cr(VI)
6-*O*-(*O*-*O*′-dilauroyl-tartaryl)-D-glucose	Hydrothermal method	2.4 ± 0.5	Surface amphiphilicity	After aerogel formation	TEOS	Atmosphere Furnace under N_2 gas atmosphere	325, NR[#], NR[#]	NR[#]	Aromatic volatile organic compound sensor
TTA	Hydrothermal method	2.1± 0.5	Surface amphiphilicity	After aerogel formation	TEOS	Autoclave	450, NR[#], NR[#]	NR[#]	lanthanide and actinide ion sensor
Sawdust	Hydrothermal method	7.28	Chemical (hydroxyl groups)	Before aerogel formation	TEOS	NR[#]	692.38, NR[#], NR[#]	43.4	Chemosensor for aniline gas detection
Organic	Hydrothermal	3.6	Chemical (covalent	After aerogel	Cellulose	Freeze	>100, 98.5,	13.6-26.2	Optical sensing of

citric acid	method		linkage; carboxyamine condensation)	formation	nanofibril	drying	0.02		glutaraldehyde
Citric acid	Hydrothermal method	3.8 ± 0.3	Chemical (coordination and self-assembly)	Before aerogel formation	$Eu(NO_3)_3$, $Tb(NO_3)_3$, thymidine	Freeze drying	NR[#], 97.6, 0.0348	47.4	Display devices, advanced sensors

#NR= Not reported; EDC= N-(3-dimethylaminopropyl)-N′-ethylcarbodiimide hydrochloride; NHS= N-hydroxysuccinimide; SCCO2= Supercritical carbon dioxide; ATP= Adenosine triphosphate; GO= Graphene oxide; CM-CNF= Carboxy-methylated-cellulose nanofibrils; TEOS= Tetraethyl orthosilicate; TTA= Thenoyltrifluoroacetone. [Sources: Wang et al. (2020); Quraishi et al. (2019); Sun et al. (2021); Yuan et al. (2020); Dolai, Bhunia, and Jelinek (2017); Dolai, Bhunia, Zeiri, et al. (2017); Ma et al. (2019); Wu et al. (2019); Zhang et al. (2020)]

2.7 Method of Formalin detection in Fish

Fish is a highly perishable commodity which get spoiled quickly. Therefore, it is very challenging to maintain freshness, texture and overall quality of fish with time. Freezing, ice cooling, chilling, etc. are some of the conventional techniques usually adopted to preserve fish with time. However, with the aforesaid techniques quality of fish is compromised by default which reflects loss of money to the fish merchants. To get rid of this loss and maximizing profit fish merchants thrives for a technique through which they can escalate shelf life of fish. They started applying harmful chemicals like sodium benzoate and FA in fish illegally (Mehta et al. 2023). Therefore, the knowledge of methods for FA detection is of high importance. The conventional as well as advance method of FA detection are discussed below.

2.7.1 *Conventional methods*

2.7.1.1 *Spectrophotometric method*

Spectrophotometric method is considered to be one of the standard method of determination of FA. The standard method of FA detection is popularly known as acetylacetone method. In this method, Nash reagent is first prepared with ammonium acetate, acetylacetone and acetic acid. As the reagent is light sensitive it is kept in dark condition and the pH of the reagent is maintained in the range of 6.0 - 6.5 by adding ammonium hydroxide (Naksen et al., 2022) or 0.1 N HCl and 0.1 N KOH (Das et al., 2018). A standard curve is made between absorbance (at 415 nm in spectrophotometer) and standard concentration of FA in Nash reagent (Das et al., 2018). The concentration of FA present can be obtained from the standard curve. Das et al. (2018) reported FA determination of different fish samples (Indian Mackerel (*Rastrelliger kanagurta*), Boyal (*Wallago attu*), Catla (*Catla catla*), Rohu (*Labeo rohita*), and Bombay duck (*Harpodon nehereus*)) using this method. The authors have prepared fish extract using trichloro acetic acid. The authors have reported 2.76 to 2.88 µg/g, 3.11 to 2.96 µg/g, 2.38 to 2.22 µg/g, 1.48 to 2.08 µg/g, and 1.81 to 2.35 µg/g of FA in Catla, Rohu, Boyal, Bombay duck, and Indian Mackerel fish respectively.

2.7.1.2 *HPLC method*

It is another widely accepted method of FA detection in fish. DNPH (2,4-dinitrophenylhydrazine) is widely used to form derivative of formaldehyde which is further formed to a specific and sensitive chromophore for detection in HPLC (Yeh et al., 2013; Hornshøj et al., 2015; Storey et al., 2015). Storey et al. (2015) have detected FA in fish through HPLC method in which they restricted the time of derivative formation to 2 min and stabilizing

buffer was added on it to increase stability of the derivative. The author have chosen three fish varieties (cod, tilapia, and basa) to perform the experiment. An average recovery and relative standard deviation (RSD) of 63 %, 66 % and 65 % and 15 %, 13 %, and 14 % was observed for cod, tilapia and basa fish respectively. Kundu et al. (2020) have performed study on frozen and fresh carp [*Labeo rohita* (Rohu) and *Catla catla* (Katla)] for the detection of FA. The derivative of formaldehyde have formed through condensation reaction of ethyl acetoacetate, ammonium hydroxide, and formaldehyde. HPLC have been performed to determine the FA content present in fish samples. The authors have reported high FA content of 23.30 and 19.66 mg/kg in Katla and Rohu fish respectively.

2.7.1.3 *GC-MS method*

It is another method of FA detection which works on the principle of chromatography. It is also considered as accurate, sensitive, and selective method of FA determination (Wahed et al., 2016). Bianchi et al. (2007) reported FA detection of 12 fish species (sea-fish, freshwater-fish and crustaceans) by this method equipped with solid phase microextraction (SPME). The derivative of fiber is prepared with pentafluorobenzyl hydroxyl amine hydrochloride which acts as sensitive chromophore for detection in GC-MS. The authors have reported FA ranges from 6.4 to 293 mg/kg and the limit of detection (LOD) and limit of quantification (LOQ) of FA 17 and 28 µg/kg respectively.

2.7.2 *Advanced methods*

2.7.2.1 *Colorimetric method*

Colorimetric method usually works on the basis of color change of substrate in which sample is deposited. Colorimetric method works on the basis of formation of derivative of FA (Costa et al., 2023). Seebunrueng et al. (2024) have developed a test kit for FA detection. The author have used the concept of Hantzsch reaction in which Nash reagent react with FA and form yellow color solution of diacetyldihydrolutidine (DDL). The development of yellow color observed under different concentration of FA solutions. The authors have reported a linear range of detection of 0.5 to 75 mg/l and LOD of 0.11 mg/l with recovery ranges from 92 to 111 %. Previously, Rovina et al. (2020) have developed a hybrid polymer film with the similar concept of color change using Nash reagent. The author have extracted RGB value from the images (showing color change) captured through smart phone and quantified the FA determination value. The author reported LOD of 5 ppm and LOQ of 16.8 ppm with recoveries ranges from 98.80 to 104.65 % of the developed method. Chutia et al. (2024) reported a qualitative detection of FA on the basis of color developed on the strip of the test kit [HiMedia's

HiRapid Formalin Test Kit (K137)]. The yellowish color developed on the strip confirms no trace of FA whereas, a green or dark bluish color represents presence of formalin.

A chemodosimeter was fabricated by Chaiendoo et al. (2018) using silver nanoclusters (AgNCs) in the presence of Tollens reagent stabilized by polymethacrylic acid (PMAA). The amine complex ($[Ag(NH_3)_2]^+$) of Ag^+ formed in the alkaline medium can be reduced to Ag^0 in presence of FA and it get deposited on AgNCs and forms silver nanoparticles (AgNPs). It results in increased particle size with change in color. The intensity is also observed to be increased. The authors have reported the linear range of this selective colorimetric assay from 30 to 50 μM and LOD of 27.99 μM.

2.7.2.2 *Fluorescence method*

Fluorescence method is another reliable method of FA determination. In this method, change in fluorescence intensity or color of specific materials are used as the methodology of detection. CDs are very popular nanomaterials which shows good fluorescent behaviour. The quenching and regaining of fluorescence behaviour of CDs is utilized to develop detection mechanism of FA (Naksen et al., 2022; Singseeta et al., 2023). Naksen et al. (2022) reported development of FA detection mechanism on the basis of silver mirror reaction. The authors have developed nitrogen doped CDs from the mixture of ethylene glycol and ammonium hydroxide and Tollens reagent is used with CDs to quench its fluorescence due to development of N-CDs-Ag^+, then the fluorescence is regained using FA as Ag^+ reduced to Ag^0. Based on the fluorescence intensity regained, a standard curve is plotted with standard concentrations of FA. The authors have reported a linear range of FA detection from 5 to 100 mg/L with LOD of 1.5 mg/L. Wongsing et al. (2023) have developed a fluorescence-based portable device to detect FA by following similar mechanism of detection as reported by Naksen et al. (2022). The authors have reported percentage recovery of 101.67 to 104.10 with relative error of -2.53 to 0.73 % for fish samples. The authors have reported a linear range of FA detection from 25 to 150 mg/L with LOD of 7.51 mg/L and LOQ of 25.04 mg/L.

Resonance light scattering (RLS) of CDs is another technique of FA detection. The mechanism behind this technique is the covalent bond (C = N) formation between FA and CDs based on Schiff base reaction which forms aggregate that enhance RLS linearly with the concentration of FA (Zhang et al., 2023). Zhang et al. (2023) reported an FA detection assay with broad linear range of detection (4 nM to 1.6 mM), LOD of 1.6 nM, recovery of 99.5 to 105.8 % and RSD of 2.5 to 6.7 %.

2.7.2.3 *Other methods*

Beside the aforesaid methods, some other important methods related to FA detection have developed by different group of researchers are discussed below.

A microsensor has developed by gold ablation on alumina substrate to detect FA in fish samples (Das et al., 2020). On the interdigitated electrodes of the substrate, nanostructured SnO_2 was deposited to make the platform ready for FA sensing. The sensor works on the principle of surface resistance. SnO_2 adsorb oxygen molecules when the sensor is exposed to air by trapping electrons from the conduction band of itself and the resistance is increased due to formation of space-charge region. Therefore, when SnO_2 exposed to a reducing gas (HCHO) the oxygen ions present at the boundaries of SnO_2 could oxidize HCHO readily and the electrons were revert back to conduction band which results in decreased resistance. The authors have reported linear range of HCHO detection from 0.5 to 5 ppm.

Torrarit et al. (2022) have developed a composite material [palladium particles (PdPs) and carbon microspheres (CMs) modified glassy carbon electrode (GCE)] for FA detection. The composite works on the basis of flow injection amperometry. The electrocatalytic performance related to oxidation of FA measures the concentration of FA through amperometry and cyclic voltammetry (CV). The authors have reported linear range of operation from 0.025 to 15.00 mmol/L and LOD of 8 µmol/L with recoveries between 96 and 105 %. A similar kind of work with different composite material made of cadmium sulphide nanoparticles (CdS) and chitosan modified GCE was reported by Baabu et al. (2020) for the detection of FA in fish. The composite works on the technique of cyclic voltammetry. The authors have reported linear range of detection from 5 to 50 mg/L and LOD of 5 mg/L.

Biosensor based detection techniques are widely accepted due to their selectivity and sensitivity towards the target material. A potentiometric enzyme (alcohol oxidase) biosensor was developed by Nurlely et al. (2021) for FA detection. The biosensor is based on succinimide-functionalized polyacrylate ion-selective membrane which performs as enzyme supporting matrix as well as pH sensitive transducer on the Ag/AgCl screen-printed electrode. Ion-ionophore complexation at the interface due to immobilized hydrogen ionophore resulted from H^+ ion transfer reaction at electrode-electrolyte interface leads the FA detection. The authors have reported a linear range of detection from 0.5 to 220.0 mM and LOD of 0.1 mM.

An electrochemical biosensor works in the basis of electron generation during interaction with the sample which results in electrochemical signals was developed by Noor Aini et al.

(2016). The signals generated was measured by electrochemical detector. Gold nanoparticles (AuNPs), chitosan and an ionic liquid (1-ethyl-3-methylimidazolium trifluoromethanesulfonate) was deposited on GCE to develop the biosensor. A wide linear range of FA (0.01 to 10 ppm) was detected by differential pulse voltammetry method. The authors have reported LOD of 0.1 ppm.

An optical fibre bundle based sensor was developed by Yasin et al. (2019) to detect FA in fish. It works on the basis of intensity of backscattered radiation (IBR) from the sample shined with red laser light at 630 nm wavelength. The authors have reported linear increase on IBR with respect to FA concentration (3 to 21 %). This FA detection method is very simple, economic, non-destructive and non-invasive.

2.8 Conclusion

It can be summarized that biopolymer based aerogel are emerging and novel materials for exploitation in food systems. These aerogel are derived basically from natural biopolymers (polysaccharides, protein, mucilage etc.). Biopolymer based aerogel are highly accepted due to their biocompatible, biodegradable, edible, renewable, and environment friendly nature. The final properties are decided by the origin, type and concentration of precursor material, method of preparation (gelation method, solvent exchange, drying method), concentration of cross-linker and surfactants etc. Limited studies on the development and comparison of corn starch based aerogel using different drying techniques are available. The existing techniques are costly and time consuming, especially the drying time is very high. In the preparation of aerogels, raw materials charges a minimal cost however, the multiple step production process charges higher amount of costs due to use of greater amount of solvents (such as ethanol, supercritical CO2, etc.). It is a challenge for the researchers as well as the industries to find an alternative way for development of aerogels. Use of a sustainable drying techniques like microwave drying, in the field of biopolymer-based aerogel development may be a good alternative. However, use of microwave drying in the field of aerogel is not well reported. Biopolymer based aerogel terms as ‘loaded’ aerogel when it serves as carrier matrix. CDs based aerogel exhibit photo luminescence behaviour with good quantum yield. CDs based aerogel have a wide range of uses due to their porous texture, optical behaviour, and sensitivity to varied stimuli (heavy metal detection, volatile gas sensing, etc.). The illegal addition of FA in food preservation especially in fish preservation is increasing significantly every day. To cope with the situation, development of a suitable method of FA detection become very important. The conventional methods of FA detection are complex, time consuming, and costly. The

advance methods like film based, test kit based FA detection strategies are competent however, CDs based aerogel have the potential to replace other methods as it exhibits superior qualities like light weight, high and rapid water absorption capability, mechanical strength, porous integrity which gives spaces for interaction, fluorescence property, visual detection, ease of operation, etc. over other materials. CDs are widely used due to their superior and versatile quality traits. The application of CDs in the field of formalin detection in food systems are available however, studies on CDs loaded aerogel in the field of formalin detection is limited. As aerogels are emerging, there is always a thrust to develop an effective, economic, and feasible way to commercialize aerogel for the benefit of food industries, application in sensing of adulteration in food products etc.

2.9 References

Abdul Khalil, H. P. S., Adnan, A. S., Yahya, E. B., Olaiya, N. G., Safrida, S., Hossain, M., Balakrishnan V., Gopakumar D. A., Abdullah C. K., Oyekanmi A.A.,& Pasquini, D. (2020). A Review on plant cellulose nanofibre-based aerogels for biomedical applications. *Polymers*, *12*(8), 1759.

Abhari, N., Madadlou, A., & Dini, A. (2017). Structure of starch aerogel as affected by crosslinking and feasibility assessment of the aerogel for an anti-fungal volatile release. *Food chemistry*, *221*, 147-152.

Ago, M., Ferrer, A., & Rojas, O. J. (2016). Starch-based biofoams reinforced with lignocellulose nanofibrils from residual palm empty fruit bunches: Water sorption and mechanical strength. *ACS Sustainable Chemistry & Engineering*, *4*(10), 5546-5552.

Agostinho, D. A., Paninho, A. I., Cordeiro, T., Nunes, A. V., Fonseca, I. M., Pereira, C., Matias A.,& Ventura, M. G. (2020). Properties of κ-carrageenan aerogels prepared by using different dissolution media and its application as drug delivery systems. *Materials Chemistry and Physics*, *253*, 123290.

Ahmadi, M., Madadlou, A., & Saboury, A. A. (2016). Whey protein aerogel as blended with cellulose crystalline particles or loaded with fish oil. *Food chemistry*, *196*, 1016-1022.

Alnaief, M., Alzaitoun, M. A., García-González, C. A., & Smirnova, I. (2011). Preparation of biodegradable nanoporous microspherical aerogel based on alginate. *Carbohydrate Polymers*, *84*(3), 1011-1018.

Alnaief, M., Obaidat, R., & Mashaqbeh, H. (2018). Effect of processing parameters on preparation of carrageenan aerogel microparticles. *Carbohydrate polymers*, *180*, 264-275.

Amaral-Labat, G., Grishechko, L., Szczurek, A., Fierro, V., Pizzi, A., Kuznetsov, B., & Celzard, A. (2012). Highly mesoporous organic aerogels derived from soy and tannin. *Green chemistry, 14(11)*, 3099-3106.

Araujo, E. J. S., Scopel, E., Rezende, C. A., & Martínez, J. (2023). Supercritical impregnation of polyphenols from passion fruit residue in corn starch aerogels: effect of operational parameters. *Journal of Food Engineering*, *343*, 111394.

Arboleda, J. C., Hughes, M., Lucia, L. A., Laine, J., Ekman, K., & Rojas, O. J. (2013). Soy protein–nanocellulose composite aerogels. *Cellulose*, *20*(5), 2417-2426.

Athamneh, T., Amin, A., Benke, E., Ambrus, R., Leopold, C. S., Gurikov, P., & Smirnova, I. (2019). Alginate and hybrid alginate-hyaluronic acid aerogel microspheres as potential carrier for pulmonary drug delivery. *The journal of supercritical fluids, 150*, 49-55.

Baabu, P. R. S., Srinivasan, P., Kulandaisamy, A. J., Robinson, J., Geevaretnam, J., & Rayappan, J. B. B. (2020). A non-enzymatic electrochemical biosensor for the detection of formalin levels in fishes: Realization of a novel comparator effect based on electrolyte. *Analytica Chimica Acta, 1139*, 50-58.

Bakierska, M., Chojnacka, A., Świętosławski, M., Natkański, P., Gajewska, M., Rutkowska, M., & Molenda, M. (2017). Multifunctional carbon aerogels derived by sol–gel process of natural polysaccharides of different botanical origin. *Materials*, *10*(11), 1336.

Baldino, L., Cardea, S., Scognamiglio, M., & Reverchon, E. (2019). A new tool to produce alginate-based aerogels for medical applications, by supercritical gel drying. *The Journal of Supercritical Fluids*, *146*, 152-158.

Betz, M., García-González, C. A., Subrahmanyam, R. P., Smirnova, I., & Kulozik, U. (2012). Preparation of novel whey protein-based aerogels as drug carriers for life science applications. *The Journal of Supercritical Fluids*, *72*, 111-119.

Bhandari, J., Mishra, H., Mishra, P. K., Wimmer, R., Ahmad, F. J., & Talegaonkar, S. (2017). Cellulose nanofiber aerogel as a promising biomaterial for customized oral drug delivery. *International Journal of Nanomedicine*, *12*, 2021–2031.

Bhartiya, P., Singha, A., Kumara, H., Jaina, T., Singha, B. K., & Dutta, P. K. (2016). Carbon dots: chemistry, properties and applications. *J Indian Chem Soc*, *93*, 1-8.

Bianchi, F., Careri, M., Musci, M., & Mangia, A. (2007). Fish and food safety: Determination of formaldehyde in 12 fish species by SPME extraction and GC–MS analysis. *Food chemistry, 100*(3), 1049-1053.

Boningari, T., & Smirniotis, P. G. (2016). Impact of nitrogen oxides on the environment and human health: Mn-based materials for the NOx abatement. *Current Opinion in Chemical Engineering*, *13*, 133-141.

Bora, A. F. M., Ma, S., Li, X., & Liu, L. (2018). Application of microencapsulation for the safe delivery of green tea polyphenols in food systems: Review and recent advances. *Food Research International*, *105*, 241-249.

Borkovec, M., & Papastavrou, G. (2008). Interactions between solid surfaces with adsorbed polyelectrolytes of opposite charge. *Current Opinion in Colloid and Interface Science*, *13*(6), 429–437.

Chaiendoo, K., Sooksin, S., Kulchat, S., Promarak, V., Tuntulani, T., & Ngeontae, W. (2018). A new formaldehyde sensor from silver nanoclusters modified Tollens' reagent. *Food chemistry, 255*, 41-48.

Chen, H. B., Wang, Y. Z., & Schiraldi, D. A. (2013). Foam-like materials based on whey protein isolate. *European polymer journal*, *49*(10), 3387-3391.

Chen, K., & Zhang, H. (2019). Alginate/pectin aerogel microspheres for controlled release of proanthocyanidins. *International journal of biological macromolecules*, *136*, 936-943.

Chen, L., Li, Y., Du, Q., Wang, Z., Xia, Y., Yedinak, E., Lou, J., & Ci, L. (2017). High performance agar/graphene oxide composite aerogel for methylene blue removal. *Carbohydrate Polymers*, *155*, 345–353.

Cheng, Y., Lu, L., Zhang, W., Shi, J., & Cao, Y. (2012). Reinforced low density alginate-based aerogels: preparation, hydrophobic modification and characterization. *Carbohydrate polymers*, *88*(3), 1093-1099.

Chutia, B. C., Borah, M. P., Bordoloi, U., Goswami, L. M., Bharadwaj, S., Borthakur, M., Sharma, P., Das, J., & Borkataki, S. (2024). Qualitative detection of formaldehyde in

challani fish obtained from selected fish markets of Nagaon, Assam, India. Discover Environment, 2(1), 26.

Ciftci, D., Ubeyitogullari, A., Huerta, R. R., Ciftci, O. N., Flores, R. A., & Saldaña, M. D. (2017). Lupin hull cellulose nanofiber aerogel preparation by supercritical CO_2 and freeze drying. *The Journal of Supercritical Fluids*, *127*, 137-145.

Comin, L. M., Temelli, F., & Saldaña, M. D. (2012a). Barley β-glucan aerogels as a carrier for flax oil via supercritical CO2. *Journal of food engineering*, *111*(4), 625-631.

Comin, L. M., Temelli, F., & Saldaña, M. D. (2012b). Barley beta-glucan aerogels via supercritical CO2 drying. *Food research international*, *48*(2), 442-448.

Comin, L. M., Temelli, F., & Saldaña, M. D. (2015). Flax mucilage and barley beta-glucan aerogels obtained using supercritical carbon dioxide: Application as flax lignan carriers. *Innovative Food Science & Emerging Technologies*, *28*, 40-46.

Costa, N. S., Maringolo, V., Brasil, M. A., Rocha, D. L., & Melchert, W. R. (2023). Online sample preparation of milk samples for spectrophotometric determination of formaldehyde. *Journal of Food Composition and Analysis, 119*, 105271.

Cristina, A., Souza, D., Dias, A. M. A., Sousa, H. C., & Tadini, C. C. (2014). Impregnation of cinnamaldehyde into cassava starch biocomposite films using supercritical fluid technology for the development of food active packaging. *Carbohydrate Polymers*, *102*, 830–837.

Dai, L., Cheng, T., Duan, C., Zhao, W., Zhang, W., Zou, X., Aspler, J.,& Ni, Y. (2019). 3D printing using plant-derived cellulose and its derivatives: A review. *Carbohydrate polymers*, *203*, 71-86.

Das, A. M., Ali, A. A., & Hazarika, M. P. (2014). Synthesis and characterization of cellulose acetate from rice husk: Eco-friendly condition. *Carbohydrate polymers*, *112*, 342-349.

Das, S., Kumar, R., Singh, J., & Kumar, M. (2020). Fabrication of microsensor for detection of low-concentration formaldehyde gas in formalin-treated fish. *IEEE Transactions on Electron Devices, 67*(12), 5710-5716.

Das, U. N., Jana, P., Dhanabalan, V., & Xavier, K. M. (2018). Detection of formaldehyde content in selected fish from three different retail markets at Mumbai. *International Journal of Current Microbiology and Applied Sciences, 7*(11), 2316-2322.

De Cicco, F., Russo, P., Reverchon, E., García-González, C. A., Aquino, R. P., & Del Gaudio, P. (2016). Prilling and supercritical drying: A successful duo to produce core-shell polysaccharide aerogel beads for wound healing. *Carbohydrate polymers*, *147*, 482-489.

De Marco, I., & Reverchon, E. (2017). Starch aerogel loaded with poorly water-soluble vitamins through supercritical CO2 adsorption. *Chemical Engineering Research and Design*, *119*, 221-230.

De Marco, I., Riemma, S., & Iannone, R. (2019). Life cycle assessment of supercritical impregnation: starch aerogel+ α-tocopherol tablets. *The Journal of Supercritical Fluids*, *143*, 305-312.

De Medeiros, T. V., Manioudakis, J., Noun, F., Macairan, J. R., Victoria, F., & Naccache, R. (2019). Microwave-assisted synthesis of carbon dots and their applications. *Journal of Materials Chemistry C*, *7*(24), 7175–7195.

de Oliveira, J. P., Bruni, G. P., El Halal, S. L. M., Bertoldi, F. C., Dias, A. R. G., & da Rosa Zavareze, E. (2019). Cellulose nanocrystals from rice and oat husks and their application in aerogels for food packaging. *International journal of biological macromolecules*, *124*, 175-184.

de Oliveira, J. P., Bruni, G. P., Fabra, M. J., da Rosa Zavareze, E., López-Rubio, A., & Martínez-Sanz, M. (2019). Development of food packaging bioactive aerogels through the valorization of Gelidium sesquipedale seaweed. *Food Hydrocolloids*, *89*, 337-350.

de Oliveira, J. P., Bruni, G. P., Fonseca, L. M., da Silva, F. T., da Rocha, J. C., & da Rosa Zavareze, E. (2020). Characterization of aerogels as bioactive delivery vehicles produced through the valorization of yerba-mate (Illex paraguariensis). *Food Hydrocolloids*, *107*, 105931.

de Souza, A. C., Dias, A. M., Sousa, H. C., & Tadini, C. C. (2014). Impregnation of cinnamaldehyde into cassava starch biocomposite films using supercritical fluid technology for the development of food active packaging. *Carbohydrate polymers*, *102*, 830-837.

Dias, A. L. B., Hatami, T., Viganó, J., de Araújo, E. J. S., Mei, L. H. I., Rezende, C. A., & Martínez, J. (2022). Role of supercritical CO2 impregnation variables on β-carotene loading into corn starch aerogel particles. *Journal of CO2 Utilization*, *63*, 102125.

Dogenski, M., Navarro-Díaz, H. J., de Oliveira, J. V., & Ferreira, S. R. S. (2020). Properties of starch-based aerogels incorporated with agar or microcrystalline cellulose. *Food Hydrocolloids*, *108*, 106033.

Dolai, S., Bhunia, S. K., Beglaryan, S. S., Kolusheva, S., Zeiri, L., & Jelinek, R. (2017). Colorimetric polydiacetylene-aerogel detector for volatile organic compounds (VOCs). *ACS Applied Materials and Interfaces*, *9*(3), 2891–2898.

Dolai, S., Bhunia, S. K., & Jelinek, R. (2017). Carbon-dot-aerogel sensor for aromatic volatile organic compounds. *Sensors and Actuators, B: Chemical*, *241*, 607–613.

Dolai, S., Bhunia, S. K., Zeiri, L., Paz-Tal, O., & Jelinek, R. (2017). Thenoyltrifluoroacetone (TTA)-Carbon Dot/Aerogel Fluorescent Sensor for Lanthanide and Actinide Ions. *ACS Omega*, *2*(12), 9288–9295.

Dong, Y., Pang, H., Yang, H. Bin, Guo, C., Shao, J., Chi, Y., Li, C. M., & Yu, T. (2013). Carbon-Based Dots Co-doped with Nitrogen and Sulfur for High Quantum Yield and Excitation-Independent Emission. *Angewandte Chemie*, *125*(30), 7954–7958.

dos Santos, P., Viganó, J., de Figueiredo Furtado, G., Cunha, R. L., Hubinger, M. D., Rezende, C. A., & Martinez, J. (2020). Production of resveratrol loaded alginate aerogel: Characterization, mathematical modeling, and study of impregnation. *The Journal of Supercritical Fluids*, *163*, 104882.

Druel, L., Bardl, R., Vorwerg, W., & Budtova, T. (2017). Starch aerogels: A member of the family of thermal superinsulating materials. *Biomacromolecules*, *18*(12), 4232-4239.

Durães, L., Matias, T., Patrício, R., & Portugal, A. (2013). Silica based aerogel-like materials obtained by quick microwave drying. *Materialwissenschaft und Werkstofftechnik*, *44*(5), 380-385.

Ehtesabi, H., Roshani, S., Bagheri, Z., & Yaghoubi-Avini, M. (2019). Carbon dots—Sodium alginate hydrogel: A novel tetracycline fluorescent sensor and adsorber. *Journal of Environmental Chemical Engineering*, *7*(5), 103419.

Erkmen, O., & Bozoglu, T. F. (2016a). In Volume 1: Microorganisms Related to Foods, Foodborne Diseases and Food Spoilage. *Food Microbiology: principles into practice*. John Wiley and Sons, Ltd.

Erkmen, O., & Bozoglu, T. F. (2016b). In Volume 2: Microorganisms in Food Preservation and Processing. *Food Microbiology: principles into practice*. John Wiley and Sons, Ltd.

Falahati, M. T., & Ghoreishi, S. M. (2019). Preparation of Balangu (Lallemantia royleana) seed mucilage aerogels loaded with paracetamol: Evaluation of drug loading via response surface methodology. *The Journal of Supercritical Fluids*, *150*, 1-10.

Favaro, S. L., de Oliveira, F., Reis, A. V., Guilherme, M. R., Muniz, E. C., & Tambourgi, E. B. (2008). Superabsorbent hydrogel composed of covalently crosslinked gum arabic with fast swelling dynamics. *Journal of applied polymer science*, *107*(3), 1500-1506.

Fonseca, L. M., Silva, F. T., Bona, N. P., Stefanello, F. M., Borges, C. D., Dias, A. R. G., & Zavareze, E. D. R. (2020). Aerogels from native and anionic corn starches loaded with Pinhão (Araucaria angustifolia) coat extract: Anti-tumor activity in C6 rat glioma cells and in vitro digestibility. *Starch-Stärke*, *72*(7-8), 1900280.

Fonseca, L. M., da Silva, F. T., Bruni, G. P., Borges, C. D., da Rosa Zavareze, E., & Dias, A. R. G. (2021). Aerogels based on corn starch as carriers for pinhão coat extract (Araucaria angustifolia) rich in phenolic compounds for active packaging. *International Journal of Biological Macromolecules*, *169*, 362-370.

Fontes-Candia, C., Erboz, E., Martínez-Abad, A., López-Rubio, A., & Martínez-Sanz, M. (2019). Superabsorbent food packaging bioactive cellulose-based aerogels from Arundo donax waste biomass. *Food Hydrocolloids*, *96*, 151-160.

Franco, P., Aliakbarian, B., Perego, P., Reverchon, E., & De Marco, I. (2018). Supercritical adsorption of quercetin on aerogels for active packaging applications. *Industrial & Engineering Chemistry Research*, *57*(44), 15105-15113.

Ganesan, K., & Ratke, L. (2014). Facile preparation of monolithic κ-carrageenan aerogels. *Soft Matter*, *10*(18), 3218-3224.

Ganesan, K., Budtova, T., Ratke, L., Gurikov, P., Baudron, V., Preibisch, I., Niemeyer, P., Smirnova, I.,& Milow, B. (2018). Review on the production of polysaccharide aerogel particles. *Materials*, *11*(11), 2144.

García-González, C. A., Alnaief, M., & Smirnova, I. (2011). Polysaccharide-based aerogels—Promising biodegradable carriers for drug delivery systems. *Carbohydrate Polymers*, *86*(4), 1425-1438.

García-González, C. A., Camino-Rey, M. C., Alnaief, M., Zetzl, C., & Smirnova, I. (2012). Supercritical drying of aerogels using CO2: Effect of extraction time on the end material textural properties. *The Journal of Supercritical Fluids*, *66*, 297-306.

García-González, C. A., Uy, J. J., Alnaief, M., & Smirnova, I. (2012). Preparation of tailor-made starch-based aerogel microspheres by the emulsion-gelation method. *Carbohydrate polymers*, *88*(4), 1378-1386.

Gawkowska, D., Cybulska, J., & Zdunek, A. (2018). Structure-related gelling of pectins and linking with other natural compounds: A review. *Polymers*, *10*(7), 762.

Gogoi, N., Barooah, M., Majumdar, G., & Chowdhury, D. (2015). Carbon dots rooted agarose hydrogel hybrid platform for optical detection and separation of heavy metal ions. *ACS applied materials & interfaces*, *7*(5), 3058-3067.

Goimil, L., Braga, M. E., Dias, A. M., Gomez-Amoza, J. L., Concheiro, A., Alvarez-Lorenzo, C., de Sousa, H. C.,& Garcia-Gonzalez, C. A. (2017). Supercritical processing of starch aerogels and aerogel-loaded poly (ε-caprolactone) scaffolds for sustained release of ketoprofen for bone regeneration. *Journal of CO2 Utilization, 18,* 237-249.

Gopakumar, D. A., Thomas, S., Owolabi, F. A. T., Thomas, S., Nzihou, A., Rizal, S., & Khalil, H. A. (2020). Nanocellulose based aerogels for varying engineering applications. *Encyclopedia of Renewable and Sustainable Materials*, *2*, p-155.

Groult, S., & Budtova, T. (2018). Tuning structure and properties of pectin aerogels. *European Polymer Journal*, *108*, 250-261.

Gullón, B., Eibes, G., Moreira, M. T., Herrera, R., Labidi, J., & Gullón, P. (2018). Yerba mate waste: A sustainable resource of antioxidant compounds. *Industrial Crops and Products*, *113*, 398-405.

Haimer, E., Wendland, M., Schlufter, K., Frankenfeld, K., Miethe, P., Potthast, A., Rosenau, T., & Liebner, F. (2010). Loading of bacterial cellulose aerogels with bioactive compounds by antisolvent precipitation with supercritical carbon dioxide. In *Macromolecular Symposia*, 294(2), 67-74.

Han, C., Li, Y. H., Qi, M. Y., Zhang, F., Tang, Z. R., & Xu, Y. J. (2020). Surface/Interface Engineering of Carbon-Based Materials for Constructing Multidimensional Functional Hybrids. *Solar Rrl*, *4*(8), 1900577.

Hatami, T., de Araújo, E. J. S., Dias, A. L. B., Mei, L. H. I., & Martínez, J. (2024). Mechanism of multicyclic β-carotene impregnation into corn starch aerogels via supercritical CO2 with mathematical modeling. *Food Research International*, *178*, 114002.

He, H., Huang, L., Zhong, Z., & Tan, S. (2018). Constructing three-dimensional porous graphene-carbon quantum dots/g-C3N4 nanosheet aerogel metal-free photocatalyst with enhanced photocatalytic activity. *Applied Surface Science*, *441*, 285-294.

He, J., He, Y., Chen, Y., Zhang, X., Hu, C., Zhuang, J., Lei, B., & Liu, Y. (2018). Construction and multifunctional applications of carbon dots/PVA nanofibers with phosphorescence and thermally activated delayed fluorescence. *Chemical Engineering Journal*, *347*, 505–513.

Hess, S. C., Permatasari, F. A., Fukazawa, H., Schneider, E. M., Balgis, R., Ogi, T., Okuyama, K., & Stark, W. J. (2017). Direct synthesis of carbon quantum dots in aqueous polymer solution: one-pot reaction and preparation of transparent UV-blocking films. *Journal of Materials Chemistry A*, *5*(10), 5187-5194.

Hornshøj, B. H., Kobbelgaard, S., Blakemore, W. R., Stapelfeldt, H., Bixler, H. J., & Klinger, M. (2015). Quantification of free formaldehyde in carrageenan and processed Eucheuma seaweed using high-performance liquid chromatography. *Food Additives & Contaminants: Part A, 32*(2), 152-160.

Hou, Y., Zhong, X., Ding, Y., Zhang, S., Shi, F., & Hu, J. (2020). Alginate-based aerogels with double catalytic activity sites and high mechanical strength. *Carbohydrate Polymers*, *245*, 116490.

Hu, B., Wang, Y., Xie, M., Hu, G., Ma, F., & Zeng, X. (2015). Polymer nanoparticles composed with gallic acid grafted chitosan and bioactive peptides combined antioxidant, anticancer activities and improved delivery property for labile polyphenols. *Journal of Functional Foods*, *15*, 593-603.

Hu, T., Xu, J., Ye, Y., Han, Y., Li, X., Wang, Z., Sun, D., Zhou, Y., & Ni, Z. (2019). Visual detection of mixed organophosphorous pesticide using QD-AChE aerogel based microfluidic arrays sensor. *Biosensors and Bioelectronics*, *136*, 112–117.

Huang, S., Li, H., Wang, M., Qian, Y., Steenland, K., Caudle, W. M., Liu, Y., Sarnat, J., Papatheodorou, S., & Shi, L. (2021). Long-term exposure to nitrogen dioxide and mortality: a systematic review and meta-analysis. *Science of The Total Environment*, *776*, 145968.

Jiménez-Saelices, C., Seantier, B., Cathala, B., & Grohens, Y. (2017). Spray freeze-dried nanofibrillated cellulose aerogels with thermal superinsulating properties. *Carbohydrate polymers, 157*, 105-113.

Jin, H., Nishiyama, Y., Wada, M., & Kuga, S. (2004). Nanofibrillar cellulose aerogels. *Colloids and Surfaces A: Physicochemical and Engineering Aspects*, *240*(1-3), 63-67.

Jing, L., Yang, S., Li, X., Jiang, Y., Lou, J., Liu, Z., Ding, Q., & Han, W. (2022). Effective adsorption and sensitive detection of Cr6+ by degradable collagen-based porous fluorescent aerogel. *Industrial Crops and Products*, *182*, 114882.

Kadokawa, J. I. (2011). Preparation of polysaccharide-based materials compatibilized with ionic liquids. *Ionic liquids, application and perspectives*, 95-114.

Kastner, H., Einhorn-Stoll, U., & Senge, B. (2012). Structure formation in sugar containing pectin gels–Influence of Ca2+ on the gelation of low-methoxylated pectin at acidic pH. *Food Hydrocolloids*, *27*(1), 42-49.

Kenar, J. A., Eller, F. J., Felker, F. C., Jackson, M. A., & Fanta, G. F. (2014). Starch aerogel beads obtained from inclusion complexes prepared from high amylose starch and sodium palmitate. *Green Chemistry*, *16*(4), 1921-1930.

Keshipour, S., & Khezerloo, M. (2017). Gold nanoparticles supported on cellulose aerogel as a new efficient catalyst for epoxidation of styrene. *Journal of the Iranian Chemical Society*, *14*(5), 1107-1112.

Khairol Anuar, N. K., Tan, H. L., Lim, Y. P., So'aib, M. S., & Abu Bakar, N. F. (2021). A review on multifunctional carbon-dots synthesized from biomass waste: design/fabrication, characterization and applications. *Frontiers in energy research*, *9*, 626549.

Kistler, S. S. (1931). Coherent expanded aerogels and jellies. *Nature*, *127*(3211), 741-741.

Kleemann, C., Schuster, R., Rosenecker, E., Selmer, I., Smirnova, I., & Kulozik, U. (2020). In-vitro-digestion and swelling kinetics of whey protein, egg white protein and sodium caseinate aerogels. *Food Hydrocolloids*, *101*, 105534.

Kleemann, C., Selmer, I., Smirnova, I., & Kulozik, U. (2018). Tailor made protein based aerogel particles from egg white protein, whey protein isolate and sodium caseinate: Influence of the preceding hydrogel characteristics. *Food Hydrocolloids*, *83*, 365-374.

Kobayashi, Y., Saito, T., & Isogai, A. (2014). Aerogels with 3D ordered nanofiber skeletons of liquid-crystalline nanocellulose derivatives as tough and transparent insulators. *Angewandte Chemie*, *126*(39), 10562-10565.

Koebel, M., Rigacci, A., & Achard, P. (2012). Aerogel-based thermal superinsulation: an overview. *Journal of sol-gel science and technology*, *63*(3), 315-339.

Koshy, R. R., Koshy, J. T., Mary, S. K., Sadanandan, S., Jisha, S., & Pothan, L. A. (2021). Preparation of pH sensitive film based on starch/carbon nano dots incorporating anthocyanin for monitoring spoilage of pork. *Food Control*, *126*, 108039.

Kundu, A., Dey, P., Bera, R., Sarkar, R., Kim, B., Kacew, S., Lee, B.M., Karmakar, S.,& Kim, H. S. (2020). Adverse health risk from prolonged consumption of formaldehyde-preserved carps in eastern region of Indian population. *Environmental Science and Pollution Research, 27*, 16415-16425.

Kuzmych, O., Allen, B. L., & Star, A. (2007). Carbon nanotube sensors for exhaled breath components. *Nanotechnology*, *18*(37), 375502.

Lavoine, N., & Bergström, L. (2017). Nanocellulose-based foams and aerogels: Processing, properties, and applications. *Journal of Materials Chemistry A*, *5*(31), 16105-16117.

Lazaridou, A., Biliaderis, C. G., & Izydorczyk, M. S. (2003). Molecular size effects on rheological properties of oat β-glucans in solution and gels. *Food Hydrocolloids*, *17*(5), 693-712.

Lee, S. C., Chiu, M. Y., Ho, K. F., Zou, S. C., & Wang, X. (2002). Volatile organic compounds (VOCs) in urban atmosphere of Hong Kong. *Chemosphere*, *48*(3), 375–382.

Leksrisompong, P., Gerard, P., Lopetcharat, K., & Drake, M. (2012). Bitter taste inhibiting agents for whey protein hydrolysate and whey protein hydrolysate beverages. *Journal of food science*, *77*(8), S282-S287.

Li, Y., Zhang, H., Fan, M., Zheng, P., Zhuang, J., & Chen, L. (2017). A robust salt-tolerant superoleophobic alginate/graphene oxide aerogel for efficient oil/water separation in marine environments. *Scientific reports*, *7*(1), 1-7.

Liu, W., Diao, H., Chang, H., Wang, H., Li, T., & Wei, W. (2017). Green synthesis of carbon dots from rose-heart radish and application for Fe3+ detection and cell imaging. *Sensors and Actuators B: Chemical*, *241*, 190-198.

Liu, Z., Tian, D., Shen, F., Nnanna, P. C., Hu, J., Zeng, Y., Yang, G., He, J., & Deng, S. (2020). Valorization of composting leachate for preparing carbon material to achieve high electrochemical performances for supercapacitor electrode. *Journal of Power Sources*, *458*, 228057.

Lopes, J. M., Mustapa, A. N., Pantić, M., Bermejo, M. D., Martín, Á., Novak, Z., Knez, Ž.,& Cocero, M. J. (2017). Preparation of cellulose aerogels from ionic liquid solutions for supercritical impregnation of phytol. *The Journal of Supercritical Fluids*, *130*, 17-22.

Lovskaya, D. D., Lebedev, A. E., & Menshutina, N. V. (2015). Aerogels as drug delivery systems: In vitro and in vivo evaluations. *The Journal of Supercritical Fluids*, *106*, 115-121.

Lu, K. Q., Quan, Q., Zhang, N., & Xu, Y. J. (2016). Multifarious roles of carbon quantum dots in heterogeneous photocatalysis. *Journal of energy chemistry*, *25*(6), 927-935.

Lu, K. Q., Yuan, L., Xin, X., & Xu, Y. J. (2018). Hybridization of graphene oxide with commercial graphene for constructing 3D metal-free aerogel with enhanced photocatalysis. *Applied Catalysis B: Environmental*, *226*, 16-22.

Lv, H., Yuan, Y., Xu, Q., Liu, H., Wang, Y. G., & Xia, Y. (2018). Carbon quantum dots anchoring MnO2/graphene aerogel exhibits excellent performance as electrode materials for supercapacitor. *Journal of Power Sources*, *398*, 167-174.

Ma, C. B., Zhang, Y., Liu, Q., Du, Y., & Wang, E. (2020). Enhanced Stability of Enzyme Immobilized in Rationally Designed Amphiphilic Aerogel and Its Application for Sensitive Glucose Detection. *Analytical Chemistry*, *92*(7), 5319–5328.

Ma, Y., Chen, X., Bai, J., Yuan, G., & Ren, L. (2019). Highly selective fluorescence chemosensor based on carbon-dot-aerogel for detection of aniline gas. *Inorganic Chemistry Communications*, *100*, 64–69.

Mahfoudhi, N., & Boufi, S. (2017). Nanocellulose as a novel nanostructured adsorbent for environmental remediation: a review. *Cellulose*, *24*(3), 1171-1197.

Mallepally, R. R., Bernard, I., Marin, M. A., Ward, K. R., & McHugh, M. A. (2013). Superabsorbent alginate aerogels. *The Journal of Supercritical Fluids*, *79*, 202-208.

Manzocco, L., Valoppi, F., Calligaris, S., Andreatta, F., Spilimbergo, S., & Nicoli, M. C. (2017). Exploitation of κ-carrageenan aerogels as template for edible oleogel preparation. *Food Hydrocolloids*, *71*, 68-75.

Marin, M. A., Mallepally, R. R., & McHugh, M. A. (2014). Silk fibroin aerogels for drug delivery applications. *The Journal of Supercritical Fluids, 91*, 84-89.

Martins, M., Barros, A. A., Quraishi, S., Gurikov, P., Raman, S. P., Smirnova, I., Duarte, A.R.C., & Reis, R. L. (2015). Preparation of macroporous alginate-based aerogels for biomedical applications. *The Journal of Supercritical Fluids*, *106*, 152-159.

Mavelil-Sam, R., Pothan, L. A., & Thomas, S. (2018). Polysaccharide and protein based aerogels: An introductory outlook.

Mehling, T., Smirnova, I., Guenther, U., & Neubert, R. H. H. (2009). Polysaccharide-based aerogels as drug carriers. *Journal of Non-Crystalline Solids*, *355*(50-51), 2472-2479.

Mehta, N. K., Pal, D., Majumdar, R. K., Priyadarshini, M. B., Das, R., Debbarma, G., & Acharya, P. C. (2023). Effect of artificial formaldehyde treatment on textural quality of fish muscles and methods employed for formaldehyde reduction from fish muscles. *Food Chemistry Advances, 3*, 100328.

Meng, G., Peng, H., Wu, J., Wang, Y., Wang, H., Liu, Z., & Guo, X. (2017). Fabrication of superhydrophobic cellulose/chitosan composite aerogel for oil/water separation. *Fibers and Polymers*, *18*(4), 706-712.

Mi, H. Y., Jing, X., Politowicz, A. L., Chen, E., Huang, H. X., & Turng, L. S. (2018). Highly compressible ultra-light anisotropic cellulose/graphene aerogel fabricated by bidirectional freeze drying for selective oil absorption. *Carbon*, *132*, 199-209.

Mikkonen, K. S., Parikka, K., Ghafar, A., & Tenkanen, M. (2013). Prospects of polysaccharide aerogels as modern advanced food materials. *Trends in food science & technology*, *34*(2), 124-136.

Mohammed, S. J., Omer, K. M., & Hawaiz, F. E. (2023). Deep insights to explain the mechanism of carbon dot formation at various reaction times using the hydrothermal technique: FT-IR, 13 C-NMR, 1 H-NMR, and UV-visible spectroscopic approaches. *RSC advances*, *13*(21), 14340-14349.

Montero-Montoya, R., López-Vargas, R., & Arellano-Aguilar, O. (2018). Volatile organic compounds in air: sources, distribution, exposure and associated illnesses in children. *Annals of global health*, *84*(2), 225.

Moradi, M., Molaei, R., Kousheh, S. A., T. Guimarães, J., & McClements, D. J. (2021). Carbon dots synthesized from microorganisms and food by-products: active and smart food packaging applications. *Critical Reviews in Food Science and Nutrition*, 1-17.

Mustapa, A. N., Martin, A., Sanz-Moral, L. M., Rueda, M., & Cocero, M. J. (2016). Impregnation of medicinal plant phytochemical compounds into silica and alginate aerogels. *The journal of supercritical fluids, 116*, 251-263.

Muthukumar, J., Selvasekaran, P., Lokanadham, M., & Chidambaram, R. (2020). Food and food products associated with food allergy and food intolerance-An overview. *Food Research International*, 109780.

Naksen, P., Jarujamrus, P., Anutrasakda, W., Promarak, V., Zhang, L., & Shen, W. (2022). Old silver mirror in qualitative analysis with new shoots in quantification: nitrogen-doped carbon dots (N-CDs) as fluorescent probes for "off-on" sensing of formalin in food samples. *Talanta, 236*, 122862.

Nešić, A., Gordić, M., Davidović, S., Radovanović, Ž., Nedeljković, J., Smirnova, I., & Gurikov, P. (2018). Pectin-based nanocomposite aerogels for potential insulated food packaging application. *Carbohydrate polymers*, *195*, 128-135.

Ni, X., Ke, F., Xiao, M., Wu, K., Kuang, Y., Corke, H., & Jiang, F. (2016). The control of ice crystal growth and effect on porous structure of konjac glucomannan-based aerogels. *International journal of biological macromolecules*, *92*, 1130-1135.

Niknia, N., Kadkhodaee, R., & Eshtiaghi, M. N. (2020). Gum tragacanth-polyvinyl alcohol aerogel for oral delivery of silymarin. *International journal of biological macromolecules, 157*, 151-157.

Nita, L. E., Ghilan, A., Rusu, A. G., Neamtu, I., & Chiriac, A. P. (2020). New trends in bio-based aerogels. *Pharmaceutics*, *12*(5), 449.

Noor Aini, B., Siddiquee, S., & Ampon, K. (2016). Development of formaldehyde biosensor for determination of formalin in fish samples; malabar red snapper (Lutjanus malabaricus) and longtail tuna (Thunnus tonggol). *Biosensors, 6*(3), 32.

Nurlely, Ahmad, M., Yook Heng, L., & Ling Tan, L. (2021). Potentiometric enzyme biosensor for rapid determination of formaldehyde based on succinimidefunctionalized polyacrylate ion-selective membrane. *Measurement, 175*, 109112.

Pantić, M., Knez, Ž.,& Novak, Z. (2016). Supercritical impregnation as a feasible techniquefor entrapment of fat-soluble vitamins into alginate aerogels. *Journal of non-crystalline solids, 432*, 519-526.

Pantić, M., Kotnik, P., Knez, Ž.,& Novak, Z. (2016). High pressure impregnation of vitamin D3 into polysaccharide aerogels using moderate and low temperatures. *The Journal of Supercritical Fluids, 118*, 171-177.

Pappalardo, J. S., Macairan, J. R., Macina, A., Poulhazan, A., Quattrocchi, V., Marcotte, I., & Naccache, R. (2020). Effects of polydopamine-passivation on the optical properties of carbon dots and its potential use in vivo. *Physical Chemistry Chemical Physics*, *22*(29), 16595-16605.

Plazzotta, S., Calligaris, S., & Manzocco, L. (2019). Structure of oleogels from κ-carrageenan templates as affected by supercritical-CO2-drying, freeze-drying and lettuce-filler addition. *Food Hydrocolloids*, *96*, 1-10.

Plazzotta, S., Calligaris, S., & Manzocco, L. (2020). Structural characterization of oleogels from whey protein aerogel particles. *Food Research International*, *132*, 109099.

Prinz, A. L., & Richter, D. J. (2022). Long-term exposure to fine particulate matter air pollution: an ecological study of its effect on COVID-19 cases and fatality in Germany. *Environmental research*, *204*, 111948.

Quraishi, S., Plappert, S. F., Grießer, T., & Liebner, F. W. (2019). Chemical versus physical grafting of photoluminescent amino-functional carbon dots onto transparent nematic nanocellulose gels and aerogels. *Cellulose*, *26*(13), 7781–7796.

Ramesh, M., Palanikumar, K., & Reddy, K. H. (2017). Plant fibre based bio-composites: Sustainable and renewable green materials. *Renewable and Sustainable Energy Reviews*, *79*, 558-584.

Robitzer, M., David, L., Rochas, C., Di Renzo, F., & Quignard, F. (2008). Nanostructure of calcium alginate aerogels obtained from multistep solvent exchange route. *Langmuir*, *24*(21), 12547-12552.

Rovina, K., Vonnie, J. M., Shaeera, S. N., Yi, S. X., & Abd Halid, N. F. (2020). Development of biodegradable hybrid polymer film for detection of formaldehyde in seafood products. *Sensing and Bio-Sensing Research, 27*, 100310.

Seebunrueng, K., Naksen, P., Jarujamrus, P., Sansuk, S., Treekamol, Y., Teshima, N., Murakami, H., & Srijaranai, S. (2024). A sensitive paper-based vapor-test kit for instant formalin detection in food products. *Food Chemistry, 451*, 139402.

Sehaqui, H., Zhou, Q., & Berglund, L. A. (2011). High-porosity aerogels of high specific surface area prepared from nanofibrillated cellulose (NFC). *Composites science and technology*, *71*(13), 1593-1599.

Selmer, I., Karnetzke, J., Kleemann, C., Lehtonen, M., Mikkonen, K. S., Kulozik, U., & Smirnova, I. (2019). Encapsulation of fish oil in protein aerogel micro-particles. *Journal of Food Engineering, 260*, 1-11.

Selmer, I., Kleemann, C., Kulozik, U., Heinrich, S., & Smirnova, I. (2015). Development of egg white protein aerogels as new matrix material for microencapsulation in food. *The Journal of Supercritical Fluids*, *106*, 42-49.

Selvasekaran, P., & Chidambaram, R. (2021). Food-grade aerogels obtained from polysaccharides, proteins, and seed mucilages: Role as a carrier matrix of functional food ingredients. *Trends in Food Science & Technology*, *112,* 455-470.

Shang, K., Yang, J. C., Cao, Z. J., Liao, W., Wang, Y. Z., & Schiraldi, D. A. (2017). Novel polymer aerogel toward high dimensional stability, mechanical property, and fire safety. *ACS applied materials & interfaces*, *9*(27), 22985-22993.

Sharma, A., & Das, J. (2019). Small molecules derived carbon dots: synthesis and applications in sensing, catalysis, imaging, and biomedicine. *Journal of nanobiotechnology*, *17*(1), 92.

Singseeta, W., Wongsing, B., Naksen, P., Jarujamrus, P., & Pencharee, S. (2023). Portable multispectral fluorometer for determination of formalin in food samples using nitrogen-doped carbon dots as the fluorescence probe. *Talanta Open, 7*, 100199.

Song, Z., Chen, X., Gong, X., Gao, X., Dai, Q., Nguyen, T. T., & Guo, M. (2020). Luminescent carbon quantum dots/nanofibrillated cellulose composite aerogel for monitoring adsorption of heavy metal ions in water. *Optical Materials*, *100*, 109642.

Stievano, M., & Elvassore, N. (2005). High-pressure density and vapor–liquid equilibrium for the binary systems carbon dioxide–ethanol, carbon dioxide–acetone and carbon dioxide–dichloromethane. *The Journal of Supercritical Fluids*, *33*(1), 7-14.

Storey, J. M., Andersen, W. C., Heise, A., Turnipseed, S. B., Lohne, J., Thomas, T., & Madson, M. (2015). A rapid liquid chromatography determination of free formaldehyde in cod. *Food Additives & Contaminants: Part A, 32*(5), 657-664.

Sun, J., Liu, Y., Wu, Z., Xu, M., Lei, E., Ma, C., Luo, S., Huang, J., Li, W., & Liu, S. (2021). Compressible, anisotropic lamellar cellulose-based carbon aerogels enhanced by carbon dots for superior energy storage and water deionization. *Carbohydrate Polymers*, *252*, 117209.

Torrarit, K., Kongkaew, S., Samoson, K., Kanatharana, P., Thavarungkul, P., Chang, K. H., Abdullah, A.F.L., & Limbut, W. (2022). Flow injection amperometric measurement of formalin in seafood. *ACS omega, 7*(21), 17679-17691.

Ubeyitogullari, A., Brahma, S., Rose, D. J., & Ciftci, O. N. (2018). In vitro digestibility of nanoporous wheat starch aerogels. *Journal of agricultural and food chemistry*, *66*(36), 9490-9497.

Ubeyitogullari, A., & Ciftci, O. N. (2016). Formation of nanoporous aerogels from wheat starch. *Carbohydrate polymers*, *147*, 125-132.

Ubeyitogullari, A., & Ciftci, O. N. (2017). Generating phytosterol nanoparticles in nanoporous bioaerogels via supercritical carbon dioxide impregnation: Effect of impregnation conditions. *Journal of Food Engineering*, *207*, 99-107.

Ubeyitogullari, A., & Ciftci, O. N. (2019). In vitro bioaccessibility of novel low-crystallinity phytosterol nanoparticles in non-fat and regular-fat foods. *Food Research International*, *123*, 27-35.

Ubeyitogullari, A., & Ciftci, O. N. (2020). Fabrication of bioaerogels from camelina seed mucilage for food applications. *Food Hydrocolloids*, *102*, 105597.

Veronovski, A., Tkalec, G., Knez, Ž.,& Novak, Z. (2014). Characterisation of biodegradable pectin aerogels and their potential use as drug carriers. *Carbohydrate polymers*, *113*, 272-278.

Vervald, A. M., Laptinskiy, K. A., Khmeleva, M. Y., & Dolenko, T. A. (2025). Toward carbon dots from citric acid and ethylenediamine, part 1: Structure, optical properties, main luminophore at different stages of synthesis. *Carbon Trends*, *19*, 100452.

Viganó, J., Meirelles, A. A., Náthia-Neves, G., Baseggio, A. M., Cunha, R. L., Junior, M. R. M., Meireles, M.A.A., Gurikov, P., Smirnova, I., & Martínez, J. (2020). Impregnation of passion fruit bagasse extract in alginate aerogel microparticles. *International journal of biological macromolecules*, *155*, 1060-1068.

Villegas, M., Oliveira, A. L., Bazito, R. C., & Vidinha, P. (2019). Development of an integrated one-pot process for the production and impregnation of starch aerogels in supercritical carbon dioxide. *The Journal of Supercritical Fluids*, *154*, 104592.

Wahed, P., Razzaq, M. A., Dharmapuri, S., & Corrales, M. (2016). Determination of formaldehyde in food and feed by an in-house validated HPLC method. *Food chemistry, 202*, 476-483.

Wan, C., Jiao, Y., Wei, S., Zhang, L., Wu, Y., & Li, J. (2019). Functional nanocomposites from sustainable regenerated cellulose aerogels: A review. *Chemical Engineering Journal*, *359*, 459-475.

Wan, C., Lu, Y., Jiao, Y., Jin, C., Sun, Q., & Li, J. (2015). Ultralight and hydrophobic nanofibrillated cellulose aerogels from coconut shell with ultrastrong adsorption properties. *Journal of Applied Polymer Science*, *132*(24).

Wang, H., Wang, C., Dang, B., Xiong, Y., Jin, C., Sun, Q., & Xu, M. (2018). Nitrogen, Sulfur, Phosphorous Co-doped Interconnected Porous Carbon Nanosheets with High Defect Density for Enhancing Supercapacitor and Lithium-Ion Battery Properties. *ChemElectroChem*, *5*(17), 2367–2375.

Wang, L., Wu, Q., Zhao, B., Li, Z., Zhang, Y., Huang, L., & Yu, S. (2022). Multi-functionalized carbon aerogels derived from chitosan. *Journal of Colloid and Interface Science*, *605*, 790-802.

Wang, M., Li, Y., Fang, J., Villa, C. J., Xu, Y., Hao, S., Li, J., Liu, Y., Wolverton, C., Chen, X., Dravid, V. P., & Lai, Y. (2020). Superior Oxygen Reduction Reaction on Phosphorus-Doped Carbon Dot/Graphene Aerogel for All-Solid-State Flexible Al–Air Batteries. *Advanced Energy Materials*, *10*(3), 1–8.

Wang, N., Hei, Y., Liu, J., Sun, M., Sha, T., Hassan, M., Bo, X., Guo, Y., & Zhou, M. (2019). Low-cost and environment-friendly synthesis of carbon nanorods assembled hierarchical meso-macroporous carbons networks aerogels from natural apples for the electrochemical

determination of ascorbic acid and hydrogen peroxide. *Analytica Chimica Acta*, *1047*, 36–44.

Wang, Ru, Lu, K. Q., Zhang, F., Tang, Z. R., & Xu, Y. J. (2018). 3D carbon quantum dots/graphene aerogel as a metal-free catalyst for enhanced photosensitization efficiency. *Applied Catalysis B: Environmental*, *233*, 11–18.

Wang, Ruixue, Li, G., Dong, Y., Chi, Y., & Chen, G. (2013). Carbon quantum dot-functionalized aerogels for NO2 gas sensing. *Analytical Chemistry*, *85*(17), 8065–8069.

Wang, Y., Chen, X., Kuang, Y., Xiao, M., Su, Y., & Jiang, F. (2019). Microstructure and filtration performance of konjac glucomannan-based aerogels strengthened by wheat straw. *International Journal of Low-Carbon Technologies*, *14*(3), 335-343.

Wang, Y., & Hu, A. (2014). Carbon quantum dots: synthesis, properties and applications. *Journal of Materials Chemistry C*, *2*(34), 6921-6939.

Wang, Y., Su, Y., Wang, W., Fang, Y., Riffat, S. B., & Jiang, F. (2019). The advances of polysaccharide-based aerogels: Preparation and potential application. *Carbohydrate polymers*, *226*, 115242.

White, R. J., Brun, N., Budarin, V. L., Clark, J. H., & Titirici, M. M. (2014). Always look on the "light" side of life: sustainable carbon aerogels. *ChemSusChem*, *7*(3), 670-689.

Wongsing, B., Promkot, S., Naksen, P., Ouiganon, S., Buranachai, C., Phooplub, K., & Jarujamrus, P. (2023). The development of the fluorescence-based portable device for lead (II) and formalin determination in food samples by using nitrogen-doped carbon dots (N-CDs). *Journal of Fluorescence, 33*(2), 565-574.

Wu, B., Zhu, G., Dufresne, A., & Lin, N. (2019). Fluorescent Aerogels Based on Chemical Crosslinking between Nanocellulose and Carbon Dots for Optical Sensor. *ACS Applied Materials and Interfaces*, *11*(17), 16048–16058.

Wu, Z. Y., Liang, H. W., Hu, B. C., & Yu, S. H. (2018). Emerging Carbon-Nanofiber Aerogels: Chemosynthesis versus Biosynthesis. *Angewandte Chemie - International Edition*, *57*(48), 15646–15662.

Xu, X., Chang, Q., Xue, C., Li, N., Wang, H., Yang, J., & Hu, S. (2022). A carbonized carbon dot-modified starch aerogel for efficient solar-powered water evaporation. *Journal of Materials Chemistry A*, *10*(21), 11712-11720.

Xu, X., Ray, R., Gu, Y., Ploehn, H. J., Gearheart, L., Raker, K., & Scrivens, W. A. (2004). Electrophoretic analysis and purification of fluorescent single-walled carbon nanotube fragments. *Journal of the American Chemical Society*, *126*(40), 12736-12737.

Yahya, E. B., Jummaat, F., Amirul, A. A., Adnan, A. S., Olaiya, N. G., Abdullah, C. K., Rizal, S., Mohamad Haafiz, M. K., & Abdul Khalil, H. P. S. (2020). A review on revolutionary natural biopolymer-based aerogels for antibacterial delivery. *Antibiotics*, *9*(10), 1–25.

Yang, L., Mukhopadhyay, A., Jiao, Y., Yong, Q., Chen, L., Xing, Y., Hamel, J., & Zhu, H. (2017). Ultralight, highly thermally insulating and fire resistant aerogel by encapsulating cellulose nanofibers with two-dimensional MoS2. *Nanoscale*, *9*(32), 11452–11462.

Yang, W., Wang, X., Gogoi, P., Bian, H., & Dai, H. (2019). Highly transparent and thermally stable cellulose nanofibril films functionalized with colored metal ions for ultraviolet blocking activities. *Carbohydrate polymers*, *213*, 10-16.

Yasin, M., Irawati, N., Zaidan, A. H., Mukti, A. T., Soegianto, A., Rosalia, D. K. P., Wardani, R.A., Khasanah, M., Kbashi, H.J., & Perego, A. M. (2019). Fiber bundle sensor for detection of formaldehyde concentration in fish. *Optical Fiber Technology, 52*, 101984.

Yeh, T. S., Lin, T. C., Chen, C. C., & Wen, H. M. (2013). Analysis of free and bound formaldehyde in squid and squid products by gas chromatography–mass spectrometry. *Journal of food and drug analysis, 21*(2), 190-197.

Yu, Z., Hu, C., Dichiara, A. B., Jiang, W., &Gu, J. (2020). Cellulose nanofibril/carbon nanomaterial hybrid aerogels for adsorption removal of cationic and anionic organic dyes. *Nanomaterials*, *10*(1), 169.

Yuan, H., Yang, G., Luo, Q., Xiao, T., Zuo, Y., Guo, X., Xu, D., & Wu, Y. (2020). A 3D net-like structured fluorescent aerogel based on carboxy-methylated cellulose nanofibrils and carbon dots as a highly effective adsorbent and sensitive optical sensor of Cr(vi). *Environmental Science: Nano*, *7*(3), 773–781.

Yun, X., Li, J., Chen, X., Chen, H., Xiao, L., Xiang, K., Chen, W., Liao, H., & Zhu, Y. (2019). Porous Fe_2O_3 modified by nitrogen-doped carbon quantum dots/reduced graphene oxide composite aerogel as a high-capacity and high-rate anode material for alkaline aqueous batteries. *ACS applied materials & interfaces, 11*(40), 36970-36984.

Zaman, A., Huang, F., Jiang, M., Wei, W., & Zhou, Z. (2020). Preparation, properties, and applications of natural cellulosic aerogels: a review. *Energy and Built Environment*, *1*(1), 60-76.

Zeng, Z., Ma, X. Y. D., Zhang, Y., Wang, Z., Ng, B. F., Wan, M. P., & Lu, X. (2019). Robust lignin-based aerogel filters: high-efficiency capture of ultrafine airborne particulates and the mechanism. *ACS Sustainable Chemistry & Engineering*, *7*(7), 6959-6968.

Zhang, F., Li, Y. H., Li, J. Y., Tang, Z. R., & Xu, Y. J. (2019). 3D graphene-based gel photocatalysts for environmental pollutants degradation. *Environmental Pollution*, *253*, 365-376.

Zhang, H., Zhang, F., & Yuan, R. (2020). Applications of natural polymer-based hydrogels in the food industry. In *Hydrogels based on natural polymers* (pp. 357-410). Elsevier.

Zhang, J., Sun, Y., Yao, Y., Huang, T., & Yu, A. (2013). Lysine-assisted hydrothermal synthesis of hierarchically porous Fe_2O_3 microspheres as anode materials for lithium-ion batteries. *Journal of Power Sources*, *222*, 59–65.

Zhang, M., Xue, J., Zhu, Y., Yao, C., & Yang, D. (2020). Multiresponsive white-light emitting aerogel prepared with codoped lanthanide/thymidine/carbon dots. *ACS Applied Materials & Interfaces*, *12*(19), 22191-22199.

Zhang, P., Wang, Y., Liu, Y., Wu, Y., & Ouyang, J. (2023). Improved stability of β-carotene by encapsulation in SHMP-corn starch aerogels. *Food Chemistry*, *406*, 135040.

Zhang, S., Fan, X., Jiang, S., Yang, D., Wang, M., Liu, T., Shao, X., Wang, S., Hu, G., & Yue, Q. (2023). High sensitive assay of formaldehyde using resonance light scattering technique based on carbon dots aggregation. *Arabian Journal of Chemistry, 16*(6), 104786.

Zhang, S., Feng, J., Feng, J., & Jiang, Y. (2017). Formation of enhanced gelatum using ethanol/water binary medium for fabricating chitosan aerogels with high specific surface area. *Chemical Engineering Journal*, *309*, 700–707.

Zhang, T., Zhang, Y., Wang, X., Liu, S., & Yao, Y. (2018). Characterization of the nano-cellulose aerogel from mixing CNF and CNC with different ratio. *Materials Letters*, *229*, 103-106.

Zhang, X., Jiang, M., Niu, N., Chen, Z., Li, S., Liu, S., & Li, J. (2018). Natural-product-derived carbon dots: from natural products to functional materials. *ChemSusChem*, *11*(1), 11-24.

Zhao, Q., Song, W., Zhao, B., & Yang, B. (2020). Spectroscopic studies of the optical properties of carbon dots: recent advances and future prospects. *Materials Chemistry Frontiers*, *4*(2), 472-488.

Zhao, S., Malfait, W. J., Guerrero-Alburquerque, N., Koebel, M. M., & Nyström, G. (2018). Biopolymer aerogels and foams: Chemistry, properties, and applications. *Angewandte Chemie International Edition*, *57*(26), 7580-7608.

Zheng, Q., Tian, Y., Ye, F., Zhou, Y., & Zhao, G. (2020). Fabrication and application of starch-based aerogel: Technical strategies. *Trends in Food Science & Technology*, *99*, 608-620.

Zheng, T., Li, A., Li, Z., Hu, W., Shao, L., Lu, L., Cao, Y.,& Chen, Y. (2017). Mechanical reinforcement of a cellulose aerogel with nanocrystalline cellulose as reinforcer. *RSC advances*, *7*(55), 34461-34465.

Zhu, F. (2019). Starch based aerogels: Production, properties and applications. *Trends in Food Science & Technology*, *89*, 1-10.

Zou, F., & Budtova, T. (2021). Tailoring the morphology and properties of starch aerogels and cryogels via starch source and process parameter. *Carbohydrate Polymers*, *255*, 117344.

Zuo, L., Zhang, Y., Zhang, L., Miao, Y. E., Fan, W., & Liu, T. (2015). Polymer/carbon-based hybrid aerogels: preparation, properties and applications. *Materials*, *8*(10), 6806-6848.